Occurrence and Global Properties of Narrow CIV lambda 1549 Absorption Lines in Moderate-Redshift Quasars

Vestergaard, Marianne

Published in:
Astrophysical Journal

DOI:
10.1086/379159

Publication date:
2003

To appear in The Astrophysical Journal, 599, December 2003
Preprint typeset using LaTeX style emulateapj v. 11/12/01

OCCURRENCE AND GLOBAL PROPERTIES OF NARROW C IV λ1549Å ABSORPTION LINES IN MODERATE-REDSHIFT QUASARS

M. Vestergaard
Department of Astronomy, The Ohio State University, 140 West 18th Avenue,
Columbus, OH 43210-1173. Email: vester@astronomy.ohio-state.edu
Accepted by ApJ, August 20, 2003

ABSTRACT

A statistical study is presented of (a) the frequency of narrow C IV λ1549 absorption lines in $1.5 \lesssim z \lesssim 3.6$ radio-quiet and radio-loud quasars, and of (b) the UV and radio properties of the absorbed quasars. The quasar sample is unbiased with respect to absorption properties and the radio-quiet and radio-loud subsamples are well matched in redshift and luminosity. A similarly high incidence ($\gtrsim$50%) of narrow C IV absorbers is detected for the radio-quiet and radio-loud quasars, and a constant ∼25% of all the quasars, irrespective of radio type display *associated* C IV absorbers stronger than $EW_{\rm rest} \geq 0.5$Å. Both radio-quiet and radio-loud quasars with narrow absorption lines have systematically redder continua, especially strongly absorbed objects. There is evidence of inclination dependent dust reddening and absorption for the radio quasars. An additional key result is that the most strongly absorbed radio quasars have the largest radio source extent. This result is in stark contrast to a recent study of the low-frequency selected Molonglo survey in which a connection between the strength of the narrow absorbers and the (young) age of the radio source has been proposed. The possible origin of these discrepant results is discussed and may be related to the higher source luminosity for the quasars studied here.

Subject headings: galaxies: active — quasars: emission lines — quasars: absorption lines — ultraviolet: galaxies

1. INTRODUCTION AND MOTIVATION

Quasar absorption lines fall into two gross categories based on their line widths, namely narrow and broad. The narrow absorption lines (NALs) have line widths less than a few hundred $\rm km\,s^{-1}$ and tend to have relatively sharp profiles. The broad absorption lines (BALs) are much more dramatic, displaying deep, broad, and smooth absorption troughs extending blueward of the emission line profile of the absorbing species; some BAL troughs are even 'detached' from the line emission profile. In the case of BALs there is no doubt that the absorbing gas is associated with the quasars as it is outflowing at sub-relativistic speeds: outflow velocities of order $-20\,000\rm km\,s^{-1}$ to $-30\,000\,\rm km\,s^{-1}$ are not uncommon, and velocities reaching $-60\,000\,\rm km\,s^{-1}$ have been detected (Jannuzi et al. 1996; Hamann et al. 1997). The NALs may be due to intervening galaxies along our line of sight to the quasar, or due to gas somehow associated with the quasar system. Gas in the quasar environment, such as a cluster, has been suggested early on to explain some of the absorbers (e.g., Weymann et al. 1979; Briggs, Turnshek, & Wolfe 1984). However, gas clearly intrinsic to the quasar is also established to produce NALs. These systems tend to cluster in velocity space within $5\,000\,\rm km\,s^{-1}$ of the emission redshift (often termed "associated NALs"; Weymann et al. 1979; Foltz et al. 1986). The strongest indications that a given NAL is associated with the quasar include: (a) time-variable absorption strengths, (b) smooth well-resolved absorption profiles that are broader than the thermal widths, (c) multiplet ratios implying partial coverage of the continuum source, and (d) high particle densities inferred from excited-state absorption lines (Barlow, Hamann, Sargent 1997), when detected. Nonetheless, NALs can still be associated without showing clear signs thereof (Hamann et al. 1997).

Early on, NALs were recognized to be key to the study of the tenuous, non-emitting gas situated between the quasars and us, but the absorption in gas associated with the quasar is also important (a) as alternative and independent probes of the central engine and the dynamics and structure therein, and (b) for understanding how quasars evolve and affect their environment on small and large scales in the process. Quasar intrinsic NALs have been suggested to originate in winds driven off a torus (e.g., Barthel, Tytler, & Vestergaard 1997) or off the accretion disk (e.g., Murray et al. 1995; Murray & Chiang 1995; Elvis 2000; Ganguly et al. 2001). Some recent thoughts on possible origins of the NALs in context of the evolution of the central host galaxy as a result of either a recent merger or a burst of star formation are discussed by Hamann et al. (2001), Baker et al. (2002), and Sabra, Hamann, & Shields (2002). Baker et al. (2002) specifically argue that dusty absorbing gas is closely related to the onset of radio activity. At least for nearby low-ionization BAL quasars, there is evidence that the BAL phenomenon may also be a temporary phase in the early evolution of the quasar (or soon after its re-ignition; e.g., Canalizo & Stockton 2001, 2002). A similar scenario has been proposed for the $z = 1.5$ radio-loud BAL quasar, FIRST J1556+3517 (Najita, Dey, & Brotherton 2000). It is also possible that some (narrow) absorbers may originate in the host galaxy itself; this has been argued for at least some Seyfert 1 galaxies (Crenshaw & Kraemer 2001). Many of the UV absorbers in Seyfert 1 galaxies also appear connected with absorption at X-ray energies (e.g., Mathur, Elvis, & Wilkes 1995; Crenshaw et al. 1999). Such a connection between UV and X-ray absorbers is also seen in BAL quasars (Brandt, Laor &

Wills 2000; Mathur et al. 2001; Green et al. 2001) and a few non-BAL quasars (e.g., Mathur et al. 1994; Brandt, Fabian, & Pounds 1996).

It has long been debated whether or not the associated NALs and the BALs are related somehow (Weymann et al. 1979) and how they may fit into the evolution of the quasars (Briggs et al. 1984; Hamann et al. 2001). A consensus is starting to appear that most associated NALs may be related to BALs, but the details of the connection differ (cf. Hamann, Korista,& Morris 1993; Hamann et al. 2001; Elvis 2000; Ganguly et al. 2001; Laor & Brandt 2002; see also Murray & Chiang 1995, 1997). If BALs and associated NALs are related, it is relevant to keep in mind that BAL outflows most likely are near-equatorial (e.g., Weymann et al. 1991). The most convincing evidence for this are likely polarization observations (e.g., Ogle et al. 1999; Schmidt & Hines 1999) combined with (a) estimates of the position angle of the radio source symmetry axis in a few nearby BALs quasars (Goodrich & Miller 1995) and (b) covering fraction arguments (Hamann et al. 1993).

The first step toward an in-depth understanding of the issues of the origin of the quasar-associated NAL gas, its connection to BAL outflows, and its importance as a probe of the central engine is to know the quasar absorption frequency, and how this frequency and the NAL and BAL properties relate to the emission properties of the quasar, if any; intervening systems will be indifferent to the intrinsic quasar properties (see § 3.2). A high fraction (50% − 70%) of low-redshift Seyfert 1 galaxies are absorbed, but BALs are not detected in these sources (e.g., Crenshaw et al. 1999; Hamann 2000). BALs are detected almost exclusively in the more luminous radio-quiet quasars (RQQs) at a frequency of 10% − 15% (e.g., Foltz et al. 1990; Hamann et al. 1993; Hewett & Foltz 2003). Relatively few radio-loud quasars (RLQs) are so far known to display BAL systems (e.g., Becker et al. 1997, 2000, 2001; Brotherton et al. 1998), although in most cases these objects may only appear mildly radio-loud owing to the absorbed optical emission yielding an artificially enhanced radio-loudness (e.g., Goodrich 2001). But BAL troughs have been detected in a few bona-fide (i.e., very radio powerful) RLQs (Gregg et al. 2000; Najita et al. 2000).

Unfortunately, the frequency of associated NALs among quasars is poorly known, especially among RQQs. While NALs have been studied almost as long as quasars themselves (Perry, Burbidge, & Burbidge 1978; Weymann, Carswell, & Smith 1981), a lot of the focus with respect to associated NALs has been on RLQs[1] and, even so, a proper census has not been made to date. Well-defined, near-complete samples provide the best basis for a proper investigation of the associated-absorption frequency of quasars with different emission properties. Such samples and their spectral data are beginning to accumulate [e.g., the Large Bright Quasar Survey (Hewett, Foltz, & Chaffee 1995); the FIRST survey (Gregg et al. 1996; White et al. 2000); the Molonglo Quasar Survey (Kapahi et al. 1998; see Baker et al. (2002) for an absorption study); and the upcoming releases of statistically well-defined and near-complete quasar samples detected in the Sloan Digital Sky Survey (e.g., Schneider et al. 2002) will undoubtedly be valuable]. Results on associated NALs in the UV are starting to appear, but mostly for low redshift quasars (Jannuzi et al. 1998; Ganguly et al. 2001; Laor & Brandt 2002) and for more distant RLQs (Baker et al. 2002).

The main goal of this paper is to provide what appears to be the first assessment of the relative C IV λ1549 absorption frequency of RQQs compared to RLQs for moderate redshift ($z \approx 2$) quasars[2]. While the sample analyzed here is neither complete nor homogeneous, it does have the advantage of being of statistically significant size and being well selected to reduce luminosity and redshift effects, as is necessary for a proper comparison of the two radio-types (§ 2). Hence, the absorption frequencies, presented here, should provide reasonable guideline values until frequencies based on larger and more complete quasar samples appear. It is also examined how the UV narrow absorption properties relate to UV and radio emission properties for clues to conditions conducive to these absorbers for different quasar types. In particular, the current data suggest (see § 4) that the relatively strong associated NALs may be the low-velocity equivalents to the dramatic BALs. This work is an extension of the preliminary results presented earlier (Vestergaard 2002; hereafter Paper I), where results for the combined sample of RLQs and RQQs were mainly presented. Here, special attention is paid to the differences in absorption properties between the two quasar radio types and between the RLQ subtypes.

The paper is organized as follows: § 2 describe the selection of the quasar samples, § 3 details the data and spectral measurements, while the results of the analysis are presented and discussed in § 4. The results are discussed in context of recent relevant studies in § 5 and § 6. A summary and the conclusions are presented in § 7.

A cosmology with $H_0 = 50$ km s^{-1}Mpc^{-1}, $q_0 = 0.0$, and $\Lambda = 0$ is used throughout, unless otherwise noted.

2. QUASAR SAMPLES

The quasar sample under study comprise 66 RLQs and 48 RQQs located at redshifts between 1.5 and 3.5; it is studied already by Vestergaard (2000), Vestergaard, Wilkes, & Barthel (2000), Vestergaard (2004a), and Paper I. A forthcoming paper will present the details of the data acquisition and processing, and the rest-frame UV spectra. The details relevant for this work are briefly summarized below and in § 3.

There are several reasons why this quasar sample is particularly useful for this investigation. First, the objects were selected for a study of the emission line profiles and, hence, were *not* selected on account of the presence of absorption lines in their spectra; the one exception is the deliberate omission of known broad absorption line quasars since the absorption can inhibit accurate measurements of the emission lines. This selection allows for an assessment

[1] This may partly be due to the combination of (i) the early debate over the reality of associated absorbers (Weymann et al. 1979; Foltz et al. 1986; cf. Young, Sargent, Boksenberg 1982; Sargent, Boksenberg, Steidel 1988), (ii) the fact that larger samples of radio-selected quasars were available for study early on, and (iii) the realization that strong NALs were somewhat common in RLQs (see Foltz et al. 1988 for discussion and review).

[2] While Richards et al. (1999) and Richards (2001) also study moderate redshift quasars, they only study the *absorbed* quasars and therefore cannot assess how commonly NALs occur among various quasar subtypes.

of the frequency of narrow absorbers in general and with respect to radio type. Second, the quasars in the two radio categories were selected to match one-on-one in luminosity and redshift to within reasonable measurement uncertainties of the absolute V-band magnitude, $\sigma(M_V) \approx 0.5$ mag and of redshift, $\sigma(z) \approx 0.01$. The RQQs and RLQs populate the same range in M_V with an average $< M_V > = -27.9$ mag, as illustrated in § 4.2. The pair-matching is used here only to ensure that the luminosity and redshift effects are minimized between the RLQs and RQQs, so not to complicate the analysis and the comparison of the two radio-subsets. Third, extensive databases of C IV broad emission line measurements (e.g., Vestergaard 2000), and of good radio data of the RLQs (see below) are available. Finally, all the rest-frame UV spectra are of relatively high-quality and are uniformly processed and measured (with reliable error estimates). Assessments can hence be made whether or not the observed absorption properties are related to UV emission properties of the quasars.

The RLQs were selected on the basis of unification models for extragalactic radio-sources to span a range in source inclination, i, with respect to our line of sight but such that the broad-line region is still visible ($i \gtrsim 44^o$; e.g., Barthel 1989). This is roughly obtained by selecting individual RLQs with a range in fractional radio-core dominance, estimated by $\log R_{5\rm GHz} = \log[S_{5\rm GHz,core}/S_{5\rm GHz,total}]$ and by $\log R_{\rm V} = \log[L_{5\rm GHz,core}/L_V]$ (e.g., Wills & Brotherton 1995), where $S_{5\rm GHz}$ is the restframe 5 GHz radio flux, $L_{5\rm GHz}$ is the luminosity at 5 GHz, and L_V is the optical rest-frame V-band continuum luminosity. RLQs are sub-classified as lobe-dominated quasars, LDQs, ($R_{5\rm GHz} < 0.5$), core-dominated quasars, CDQs ($R_{5\rm GHz} \geq 0.5$), compact steep-spectrum quasars, CSSs ($R_{5\rm GHz} < 0.5$ and the largest linear size[3] of the radio emission (LIN) is 25 kpc or less in a cosmology with $H_0 = 50$ km s^{-1}Mpc^{-1}, $q_0 = 0.5$, and $\Lambda = 0$; see footnote 4), and giga-hertz peaked spectrum quasars, GPS (compact [$\lesssim 1$ kpc] sources with convex radio spectrum peaking between 500 MHz and 10 GHz; O'Dea 1998). The LDQs are commonly interpreted to be viewed at relatively larger inclination angles than the CDQs; CDQs are believed to be viewed almost face-on ($i \lesssim 5^o - 10^o$). To avoid the possible effects of Doppler boosted (i.e., beamed) optical-UV continuum emission on the emission line properties the most strongly core-dominated quasars were selected against by omitting the known highly variable objects (at optical and radio energies), i.e., blazars. Final selection criteria were imposed to ensure that the RLQs are accessible from the Very Large Array (VLA) and are observable at the Palomar Hale 5 m telescope (i.e., $V \lesssim 19$ mag). The RQQs were selected from Hewitt & Burbidge (1993) to match the RLQs in M_V and z as described above. Unfortunately, no inclination estimator is available for the RQQs, so a similar sub-distribution in i can not be selected.

3. DATA

Rest-frame UV spectra for most of the RLQs are presented by Barthel, Tytler, & Thomson (1990). The remaining quasars were observed mainly at the Multi-Mirror Telescope (MMT). The spectra commonly cover rest-frame wavelengths ∼1000Å to ∼2100Å with a spectral resolution of ∼3.5Å to ∼5Å. Shorter exposures of many of the Barthel et al. quasars were repeated at the MMT (a) to ease the combination of the red and blue subspectra, (b) to extend these spectra to the atmospheric cutoff (∼3200Å), and (c) to provide a better flux calibration, which for some spectra is less accurate. The spectra were not corrected for Galactic extinction. This correction is typically within the uncertainty in the absolute flux calibration, since these data are not spectrophotometric. High quality Very Large Array radio maps at 1.4 GHz, 5 GHz, and 15 GHz are available for most of the RLQs (Barthel et al. 1988; Lonsdale, Barthel, & Miley 1993; Barthel, Vestergaard, & Lonsdale 2000) and fluxes are available for many of the quasars at 178 MHz or 159 MHz (Spinrad et al. 1995) and 408 MHz (Colla et al. 1970, 1972, 1973; Large et al. 1981; Wright & Otrupcek 1990).

3.1. *Spectral Measurements*

A power-law continuum ($F_\lambda \propto \lambda^{\alpha_\lambda}$) was fitted to virtually line-free regions in the spectra (see e.g., Vestergaard & Wilkes 2001). For estimates of the continuum uncertainty and its effect on other spectral measurements, the continuum level and slope were varied to the four extremes permitted by the noise in the data (i.e., the minimum, the maximum, the bluest slope, and the reddest slope). For each of these five continua the C IV emission line shape was reproduced with a smooth fit (using 2 – 3 Gaussian profiles), which eliminates noise spikes and narrow absorption lines superposed on the emission line profile. This smooth profile fit to the best fit continuum is very suitable as the local "continuum" level for the absorption lines. The emission line width, FWHM(C IV), (used in § 6) was measured directly on this smooth profile, reducing measurement errors. The FWHM uncertainty was estimated from the FWHM measurements of the profile fit made to the four extreme continuum settings.

A semi-automated absorption line search algorithm was employed, but all the data and measurements were visually inspected and confirmed. First, an extensive list of candidate C IV $\lambda\lambda$1548,1550 absorption line positions was interactively generated from the spectra in the observed frame. To minimize omissions, candidate absorbers with line peaks deviating more than $\gtrsim 1.5\sigma_{\rm rms}$ ($\sigma_{\rm rms}$ is the local spectrum *rms* noise) from the local continuum were then selected; most candidates with smaller peaks are clearly noise. This interactive search eliminates the predominant part of the noise spikes, which the human eye can more easily identify than an algorithm. Thereafter, the algorithm searches among these pre-selected candidate λ1548 and λ1550 transitions for C IV doublet lines satisfying the following criteria:

1. The peak of the λ1550.77 transition, at least, is greater than $1.5\sigma_{\rm rms}$.

2. The *observed* equivalent width $EW_{\rm obs} \geq 0.5$Å of each system/blend

[3] The linear size constraint for a steep spectrum source to be called 'CSS' is not uniform in the literature. CSSs are defined here to have a radio source extent less than 25 kpc in a cosmology with $H_0 = 50$ km s^{-1}Mpc^{-1}, $q_0 = 0.0$, and $\Lambda = 0$ to allow a direct comparison with the Baker et al. (2002) study in § 5.

3. The measured restframe separation of candidate doublet lines have $\Delta\lambda_{\rm separation,rest} = \Delta\lambda_{\rm doublet} \pm \frac{1}{2}$ resolution element, where the C IV doublet separation is $\Delta\lambda_{\rm doublet} = 1550.77 - 1548.20$Å $= 2.57$Å.

4. Rest EW doublet ratio ($\lambda1550/\lambda1548$) is in the range: $0.8 - 2.2$

5. Rest EW of each doublet is at least 3 times the detection limit, $\sigma_{\rm det}$

6. The doublet FWHMs generally match to within the resolution ($\sim$200$-$300 km s^{-1})

The FWHM criterion is not strictly enforced due to resolution/blending effects and measurement uncertainties; extensive tests show that this does not seriously affect the list of absorption candidates. Besides, the final visual inspection of the absorbers identifies clearly unrealistic or unreliable absorbers, which may have survived the filtering. The margins in $\Delta\lambda_{\rm separation,rest}$ (item 3) and EW doublet ratio (item 4) were adopted to allow for blending and resolution effects. The imposed value ranges were determined from spectra with clear presence of C IV narrow absorption doublets. The EW detection limit ($\sigma_{\rm det}$) is determined as the integrated local continuum rms noise (normalized to the local continuum level) across a single resolution element. This yields an absolute minimum detection limit. The EW is measured by integrating across the identified absorption profile of the C IV doublet. This is done because the spectral resolution and relative weakness of some of the absorption lines do not warrant employment of Gaussian fitting for line measurements. Some of the absorption lines are clearly blended at the resolution of these data and they may appear as a single absorption line. Therefore, such strong absorption blends, commonly with $EW_{\rm rest} > 1.0$Å and easily identified by eye, were not subjected to the above-listed selection criteria. The search for NALs were deliberately stopped at the restframe wavelength $\sim$1420Å to avoid the increasing probability of contamination by Si IV absorbers and other lower-redshift, intervening galaxy and/or cluster absorption. Notably, criterion 5 above ensures that each C IV NAL is detected with a confidence $\geq 3\sigma$ (i.e., the confidence in the detection is at the $\geq 99.95\%$ level). The completeness level is determined in § 3.3.

3.2. *Identification of Associated Systems*

Unfortunately, for most of the objects (except Q1726+344; see below) it cannot be firmly established that a given NAL is associated with the quasar based on the criteria listed in the introduction, since only single-epoch, moderate resolution data are available. Ideally, intervening C IV absorbers can be identified by searching for absorption lines by other species, such as Mg II, at the same redshift of the individual C IV absorbers. This is only possible in a very limited number of objects for which Mg II appears in the spectral window. Fortunately, most of the intervening absorption lines are anticipated to be relatively weak and therefore to be eliminated by the primary 0.5 Å $EW_{\rm obs}$ cutoff. Savage et al. (2000) find the strongest C IV absorption lines due to Milky Way gas detected in quasars to have $EW_{\rm obs} \lesssim 0.9$Å. The likelihood that any of the strong absorption systems ($EW_{\rm rest} \geq 1$Å) are intervening is considered to be rather small. Hence, it is fair to assume that the stronger an absorption line is, the more probable is its association; the discussion in § 4 confirms this. Note that not all the weak absorbers (e.g., with $EW_{\rm rest} < 1$Å) are per se intervening. A characteristic property of unrelated, intervening systems to bear in mind is that they should scatter evenly in redshift (up to the emission redshift) and they do not typically exhibit trends with the quasar properties[4].

Barthel et al. (1990) identified a number of absorption systems of different species in the spectra of their RLQs. While all the narrow C IV absorption lines are measured independently in this study, a cross-check was made with the Barthel et al. results to eliminate the intervening absorbers identified by them; only a few (six) such absorbers were to be eliminated (corresponding to 6.5%±1.5% of the originally identified systems). The C IV systems with identified UV transitions of, for example, Mg I λ2853, Mg II $\lambda\lambda$2796, 2804, Al II λ1671, Si IV $\lambda\lambda$1394, 1403, and/or some of the many UV Fe II and Si III transitions (e.g., Barthel et al. 1988; Savage et al. 2000) at the same absorption redshift were considered to be intervening. The two high-velocity NALs of Q2222+051 and Q2251+244 are part of systems with additional Al II, Al IIIλ1857, Si IV, and/or C II transitions, but are here considered to be intrinsic given their large strengths, $EW_{\rm rest} > 1$Å. The C IV absorbers with N V λ 1240 at the same absorber redshift must be associated with the quasar given the high level of ionization (e.g., Weymann et al. 1979; Hamann 2000; Savage et al. 2000). (Notably, while high-density absorbers may display mostly low-ionization transitions, this ionization cut will not significantly select against such absorbers, since they also tend to display strong lines with $EW_{\rm rest} \gtrsim$ 1Å). Hence, the incidence of intervening absorbers should be reduced for the RLQs in this analysis. If the RLQ fraction of intervening absorbers is typical also for RQQs, then 4 of the NALs detected in the RQQ spectra (or 5% of the entire NAL sample) are statistically expected to be intervening (but not identified as such).

While a few intervening systems may remain, it is anticipated that their inclusion will not significantly affect the results of the analysis, because (a) the samples of quasars and absorbers are large, and (b) this study is of a statistical nature. In addition, even if the ensemble of the weak absorbers (or bulk thereof) are unrelated to the quasars their properties (e.g., frequency, strength, velocity) are expected to be indifferent to varying quasar emission properties anyway, as noted above (see also footnote above). In

[4] A possible exception is that of dusty damped Lyman-α absorption (DLA) systems with detectable metal lines, which will redden the quasar spectrum. It may appear that intervening dusty DLAs can lead one to erroneously conclude that the frequency and strength (EW) of absorbers increase with dust reddening (as is, in fact, seen for this sample; discussed in § 4). However, this is not very likely. The reasons are that (1) the incidence of DLAs is very low (by a factor $\sim$0.04; Table 12.1 by Peterson 1997) compared to C IV narrow absorbers (intrinsic and intervening), and (2) DLAs have rather low metal abundances, resulting in typically weak C IV absorbers (*observed* equivalent width $\lesssim$1Å; e.g., Prochaska et al. 2003). Therefore, very few, if any, intervening C IV NALs associated with DLA systems are expected in the current sample of absorbers (<4 absorbers) which will not adversely affect the results of this study.

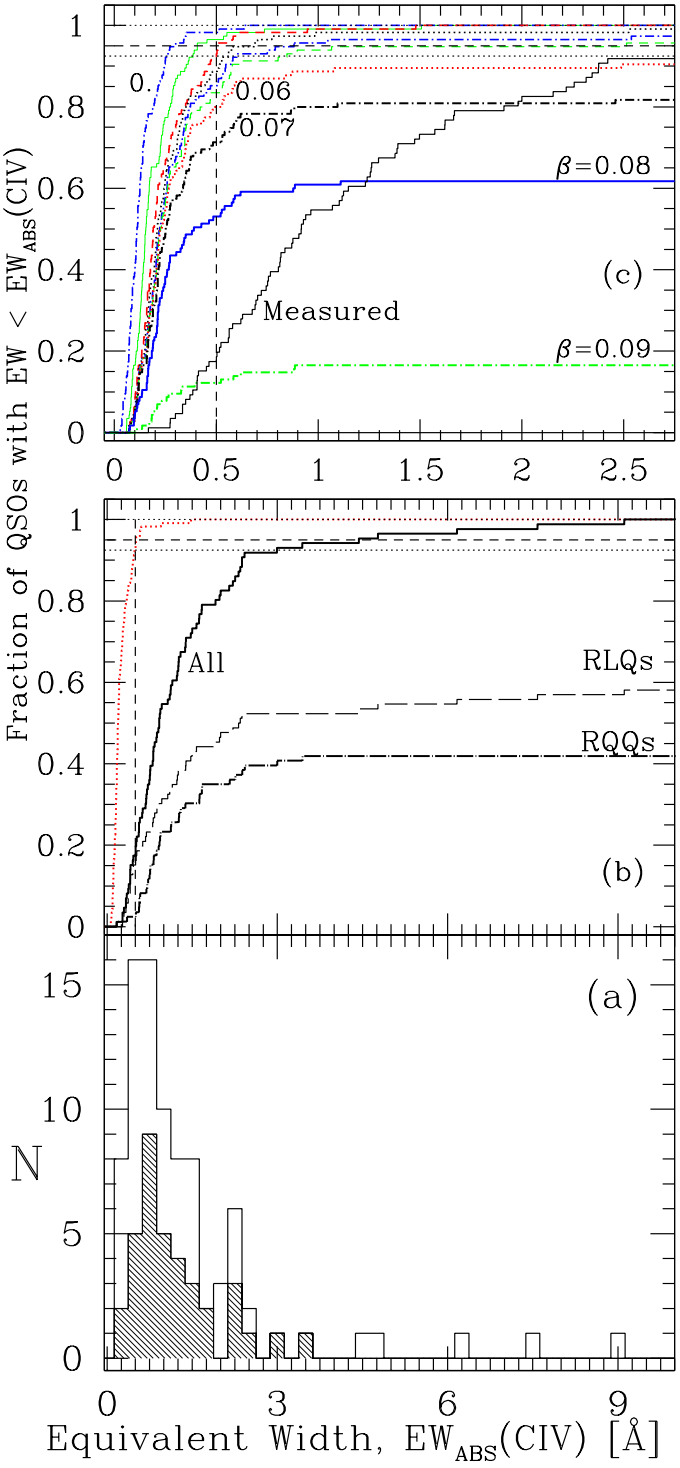

FIG. 1.— Distributions of restframe $EW_{\rm abs}$(C IV). (*a*): Restframe $EW_{\rm abs}$ distribution of the C IV doublet for the sample of absorbed quasars (solid open histogram); the RQQ subset is shown shaded. (*b*): Cumulative distribution of the measured $EW_{\rm abs}$(C IV) (heavy solid curve) is compared with the cumulative distributions of the NALs detected in the RLQs (long dashed) and RQQ (dot-dashed) subsamples. The 3σ detection limit for $\beta = 0.02$ (heavy dotted curve; see below) is shown for comparison. Vertical and horizontal lines are as in panel (c). (*c*): Cumulative distribution of the 3σ restframe EW detection limit for different β values. The leftmost curve (dot-dashed) is the distribution for $\beta = 0.0$. Going from left to right the β-value increases by 0.01. The distributions for $\beta = -0.01, -0.02$ are essentially the same as those for $\beta = 0.01, 0.02$, respectively, and are therefore not shown for clarity. However, the completeness limits for $\beta < -0.02$ stay rather high (see e.g., Fig. 7) contrary to those shown for $\beta > 0.02$. The cumulative distribution of the measured $EW_{\rm abs}$(C IV) of all the quasars is shown for comparison (labeled 'Measured'). The 92.5% and 95% completeness levels are marked by the dotted and dashed horizontal curves, respectively. The 3σ detection limit measured (in a resolution element) to a completeness level of ∼95% within $|\beta| < 0.02$ is $EW_{\rm rest} = 0.5$Å (dashed vertical line).

the following, it will be assumed that the narrow absorbers are intrinsic to or associated with the quasars, unless otherwise noted.

For one RLQ, the CSS quasar Q1726+344, Ma (2002) detected a newly developed mini-BAL; only intervening absorption was detected here. Variable absorption is a clear indication that the absorber is associated with the quasar (§ 1). The rest EW = 2Å and velocity shift = $-6000\,{\rm km\,s^{-1}}$, measured by Ma (2002), are thus adopted in this work for comparison.

3.3. *Absorber Measurements and Completeness Limits*

In the following, all EWs are restframe measurements of the C IV absorption doublet. Table 1 lists the UV properties of the absorbed quasars and their absorbers, and Table 2 lists the basic properties of the unabsorbed objects. Figure 1 shows the EW distributions of the individual C IV absorbers and the spectral detection limits, as explained next.

It is evident from Figure 1a that while the absorbers span a large range in strength, most have EWs $\lesssim 3$ Å.

The NALs in RLQs and RQQs generally distribute similarly, with the noticeable exception that only RLQ NALs are detected at $EW > 4$Å.

In Figure 1b the cumulative distribution of detected NALs is compared to the individual distributions of RLQ and RQQ absorbers. The dotted curve represents the cumulative distribution of the $3\,\sigma$ detection limit of NALs within $6000\,\mathrm{km\,s^{-1}}$ of the emission line redshift, and shows a 95% completeness level of NALs with $EW \geq 0.5$Å (see below). Evidently, only a tiny fraction of the RQQ absorbers are below the 95% completeness limit.

Figure 1c shows the cumulative distributions of the $3\,\sigma$ EW detection limits measured for different absorber velocities (parameterized by β) in the spectra of all absorbed and unabsorbed quasars. The absorber velocity is conventionally defined as $v = \beta c$, where $\beta = (r^2-1)/(r^2+1)$ and $r = (1+z_{\rm em})/(1+z_{\rm abs})$ (Weymann et al. 1979; Peterson 1997) and c is the speed of light. However, in this work $v = -\beta c$ is adopted such that a negative velocity (intuitively) corresponds to blueshifted absorption velocities. Only distributions for positive β values are shown in Figure 1c for clarity. The distributions for $\beta = -0.01, -0.02$ are essentially the same as those for $\beta = 0.01, 0.02$, respectively. The cumulative distributions show that the sensitivity of the data toward detecting NALs (at the $3\,\sigma$ significance) within $|\beta| \leq 0.02$ drops below 95% at $EW \approx 0.5$Å (vertical dashed line). In other words, associated NALs with $EW \geq 0.5$Å are $\gtrsim 95$% complete. For increasing β-values, the cumulative distributions shift to higher EWs and lower fractional completeness. A similarly high level of completeness cannot be achieved at all β values, partly owing to differences in signal-to-noise levels. Furthermore, at the highest β values ($\beta \geq 0.06$) the distributions do not reach 100% because the spectra could not all be measured at these β values. More specifically, at $\beta = 0.08$ (0.09), only ∼62% (∼17%) of the spectra could be measured. Nevertheless, the completeness level of $EW \geq 0.5$Å absorbers is still high (≥70%) for $\beta \leq 0.07$. The $\beta < 0$ cumulative distributions maintain a rather high completeness (>85% for $-0.09 \leq \beta \leq 0$), contrary to the distributions for $\beta > 0.02$. The completeness level of $EW \geq 0.5$Å NALs as a function of β is discussed in relation to the measured absorbers in § 4.4. Part of the cumulative distribution of detected absorbers is also shown in Figure 1c for comparison. This shows that more than 80% of the absorbers have EWs above the 0.5Å completeness limit.

4. RESULTS AND DISCUSSION

As described in § 1, a basic census of the associated-absorption frequency among distant quasars is poorly known, particularly among RQQs. Also, little is known about which quasar properties are favored or evaded for objects with strong (associated) NALs and how these properties compare for the two radio types. In the following, these issues are addressed with the current data. In addition, the dependence on radio source inclination (§ 4.3), and the velocity distribution of the NALs (§ 4.4) are discussed.

4.1. *Frequency of Occurrence*

Table 3 lists the fraction of absorbed quasars grouped in various ways, and Table 4 contains the absorber frequency among the absorbed quasars only. As pointed out in § 3.3 the most complete subset of NALs are at $\beta \leq 0.07$ and have $EW \geq 0.5$Å. To allow a more direct and quantifiable comparison with future quasar absorption studies, most of the statistics in Tables 3 and 4 are therefore limited to this most complete subset. If all absorbers are counted the frequencies would in places increase by a few per cent. This is mostly within the counting errors.

In Tables 3 and 4, statistics are listed for various subdivisions of the full quasar sample (col. 1): "All QSOs" (RLQs+RQQs), RQQs, RLQs, and the subgroups of RLQs: CDQs, LDQs, CSSs, and GPSs, defined in § 2; the size of each of these samples is in col. 2. Columns 3 to 5 list numbers and frequencies for various NAL velocity bins, as marked. Table 3 is divided into three sections (top, middle, bottom) according to the absorption strength. In particular, the statistics in the top section are based on all NALs with any detected EW (col. 3, left) and on individual NALs with $EW \geq 0.5$Å (col. 3, right; cols. 4 and 5). Table 4 is structured similarly to Table 3, except that the statistics of weak absorbers are omitted.

When counting all detected absorbers (all EWs) more than half of the quasars have NALs (Table 3; note that this fraction is ≳60% if all the intervening systems are included). This is comparable to the frequency (∼50 − 70%) observed among Seyfert 1 galaxies (Crenshaw et al. 1999), and shows how common this phenomenon is. This frequency is higher than that seen for the Bright Quasar Survey (BQS; $z < 0.5$) quasars studied by Laor & Brandt (2002) (40% NALs and ∼10% BALs). About 25% of the quasars have associated NALs ($EW \geq 0.5$Å; Table 3; note, this also holds when restricted to $EW \geq 1$Å, the commonly adopted division between intrinsic and intervening absorption (§ 3)). Ganguly et al. (2001) find a similar frequency of associated NALs ($15/59 \approx 25\%$ ±7%) among their sample of $z \lesssim 1$ quasars, while Baker et al. (2002) find a very high fraction of associated NALs (with $0.3\text{Å} \leq EW \leq 5.2\text{Å}$) in their RLQ sample (50% ±17% at $0.7 \leq z \leq 1.0$; 90% ±21% at $1.5 \leq z \leq 3.0$; see § 5 for discussion of the Baker et al. results). However, in reality, a direct comparison of the incidence of absorbers with the Ganguly et al. study is non-trivial as there is only a small common range in EW of the detected absorbers between the two samples: the current sample is incomplete at $EW < 0.5$ Å and contain a large number of relatively strong absorbers (≳1 Å), while the Ganguly et al. absorbers are mostly weaker than 1 Å. In the common EW range from 0.5 Å to 1 Å (summed per quasar) of associated (i.e., low-velocity) C IV NALs, Ganguly et al. find 4 absorbed quasars out of 59, or ∼7% ±3%. In comparison, the current sample has 4/114 quasars with such associated weak absorbers (i.e., $3.5\% \pm 1.7\%$). While this may appear to suggest a marginal difference in incidence, both samples are subject to small number statistics and strong conclusions based thereon are cautioned.

The RQQs appear slightly less frequently absorbed than RLQs, but their frequencies are consistent within the counting errors; this also holds when considering the low and high velocity absorbers separately (Table 3). Even if broad absorption lines (BALs) are also counted, these fre-

quencies may not change much because the BAL fraction[5] is relatively low for both RQQs and RLQs and the counting errors are at the level of the BAL fraction or larger. The RLQs and RQQs only exhibit apparent differences in the frequency of weak, low-velocity (i.e., associated) NALs. However, this may not be real since a larger number of NALs with EW below the 0.5 Å completeness limit occur among RLQs than among RQQs (Fig. 1b).

Among the subtypes of RLQs, the CDQs and CSSs are typically equally absorbed within the errors (Table 3; top section). The LDQs stand out by having significantly higher occurrence of low-velocity NALs (80% ±23%) relative to CDQs and CSSs ($\gtrsim$ 20%). For the strongly absorbed quasars there is a difference in absorption frequency between the LDQs and CDQs at the $\sim 1\,\sigma$ level (Table 3; middle section). This is seen both among the low velocity absorbers ($v \leq 5000\,\mathrm{km\,s^{-1}}$; col. 4) and in the sample of $v \leq 21\,000\,\mathrm{km\,s^{-1}}$ absorbers (col. 3). But, the high velocity LDQ and CDQ absorbers are different at the $\sim 2\,\sigma$ level (col. 5). Differences are also seen among the weakly absorbed LDQs and CDQs at the $\geq 1.5\,\sigma$ level (col. 3; bottom section). Furthermore, Table 3 shows that CDQs tend to have more weakly absorbed objects than the LDQs (col. 3). Most of this difference occur at high velocities (col. 5). The statistics for the weakly absorbed quasars should, however, be treated with caution since the subset of EW <0.5Å absorbers is incomplete (§ 3.3).

It is evident from Table 4 that most of the absorbers in any quasar subgroup are at low-velocity (i.e., likely associated; col. 4), especially the strong absorbers. Again, the frequency of low and high velocity absorbers, respectively, are similar between the RLQ and RQQ subgroups. This holds for the complete NAL sample ($EW \geq 0.5$Å) and for the strong ones alike. Only the frequency of strong absorbers in LDQs and CDQs are different: all strongly absorbed ($EW \geq$1Å) CDQs have associated NALs only.

To summarize, RLQs and RQQs exhibit similar absorption frequencies both at high and low absorber velocity, respectively. Among the RLQs, the LDQs are by far the most frequently absorbed in general. Also, LDQs tend to be the most *strongly* absorbed. These strong absorption systems mostly have velocity shifts less than $5000\,\mathrm{km\,s^{-1}}$ from the emission redshift. This will be discussed in section 4.3. The CSS quasars are discussed in § 5.

A final comment is in place. For a large, heterogeneous sample of absorbed quasars Richards et al. (1999) find marginal fractional excesses of C IV λ1549 NALs in (a) RQQs compared to RLQs, and in (b) FSS ($\simeq$ CDQ) quasars relative to SSSs ($\simeq$ LDQs), reaching velocities of $-30\,000\,\mathrm{km\,s^{-1}}$ and $-25\,000\,\mathrm{km\,s^{-1}}$, respectively. Richards (2001) confirms these findings to be marginal by including a more homogeneous data set of RLQs. Although the relative frequencies of high-velocity ($-5\,000\mathrm{km\,s^{-1}}$ to $-21\,000\,\mathrm{km\,s^{-1}}$) absorbers seem to support the above-mentioned excesses (column (4) in Table 4, top), strong conclusions based thereon are, unfortunately, premature for two reasons: (1) this quasar sample is incomplete and the high-velocity absorption results are based on small number statistics, especially for the RLQ subgroups, and (2) Richards et al. (1999) use an advanced Monte-Carlo type of normalizing algorithm in determining the relative frequency of absorbers at a given velocity for each sample, while a simple ratio is used here. The nature of the sample studied here (item 1) does not warrant such an elaborate analysis. The results of Richards et al. (1999) and Richards (2001) will therefore not be discussed further. While the findings by these authors are indeed tantalizing, to properly address these issues, complete, homogeneous, and well-selected samples are required.

4.2. *Properties of Quasars with NALs*

The distributions of UV continuum slopes, $\alpha_{\mathrm{UV},\lambda}$ ($F_\lambda \propto \lambda^{\alpha_\lambda}$) and the absolute magnitude, $\mathrm{M_V}$, are shown in Figure 2 for the quasars with and without detectable C IV λ 1549 narrow-line absorption, respectively. "Unabsorbed" quasars (note, one BAL quasar is included here) have on average a slope, $<\alpha_{\mathrm{UV}}> = -1.99$ (median = −1.89; standard deviation, $\sigma_{\mathrm{std}} = 0.64$), while the absorbed quasars in Figure 2 have $<\alpha_{\mathrm{UV}}> = -1.59$ (median = −1.62; $\sigma_{\mathrm{std}} = 0.64$). When confined to the absorbers above the 95% completeness limit of 0.5Å the absorbed quasars are slightly redder on average ($<\alpha_{\mathrm{UV}}> = -1.47$; median = −1.46; $\sigma_{\mathrm{std}} = 0.60$). Although the average slopes only differ at the $1\,\sigma$ level, Kolmogorov-Smirnov (K-S) tests confirm that the continuum slope distributions of absorbed and unabsorbed quasars are statistically different at the 99.95% confidence level or higher. Note, how much more the absorbed quasars scatter in continuum slope, in clear contrast to the unabsorbed sources; barring a few outlying unabsorbed RQQs. Notably, most of the quasars are more luminous than $M_V = -27$ mag, inconsistent with the prediction by Møller & Jakobsen (1987) that no associated absorbers should be seen for quasars more luminous than this value. About 25% of these luminous quasars have strong ($\gtrsim$1Å), associated NAL systems (Table 3; middle section).

Figures 3 and 4 illustrate how the total absorption strength for each object distribute with the quasar properties: $\alpha_{\mathrm{UV},\lambda}$ (Fig. 3a, c), M_V (Fig. 3b, d), and the 1550Å monochromatic continuum luminosity, $L_{\mathrm{cont}}(1550\text{Å})$ (Fig. 4). Table 5 lists the Spearman's correlation rank and the probability (P) that no correlation is present. The total strength (i.e., restframe EW) of the C IV NALs in each quasar in the combined sample of RLQs and RQQs correlates strongly with α_{UV} (Spearman's rank, r = 0.53) with a P <0.1% probability of occurring by chance (Fig. 3a, c). Thus, more strongly absorbed objects tend to have redder continua. The RLQs dominate this relationship (Table 5). The RQQs exhibit a weaker and less significant trend (see below); they clump[6] around $\alpha_\lambda \approx -1.5$ (Fig. 3a). Little difference is seen when individual absorbers with $EW < 0.5$Å (the 95% completeness limit) are omitted. These trends are consistent with a larger dust reddening in objects subject to stronger NALs. Notably, the RQQs with BALs or mini-BALs have some of the reddest UV continua indicating they are subject to

[5] Among optically selected samples ∼10% − 15% of the quasars are BALs (e.g., Foltz et al. 1990; Goodrich 2001; Hewett & Foltz 2003). The FIRST survey has identified (Becker et al. 2001) a similar fraction (∼10%) of BALs among bona-fide RLQs (i.e., the radio-loudness, $R^* = L_{\mathrm{radio}}/L_{\mathrm{optical}} > 10$), although most of the detected BAL quasars are radio-intermediate sources ($1 \leq R^* \leq 10$).

[6] This may be due to our inability to select RQQs with a range of source inclinations (§ 2), since inclination and absorption strength are likely related, as discussed in § 4.3.

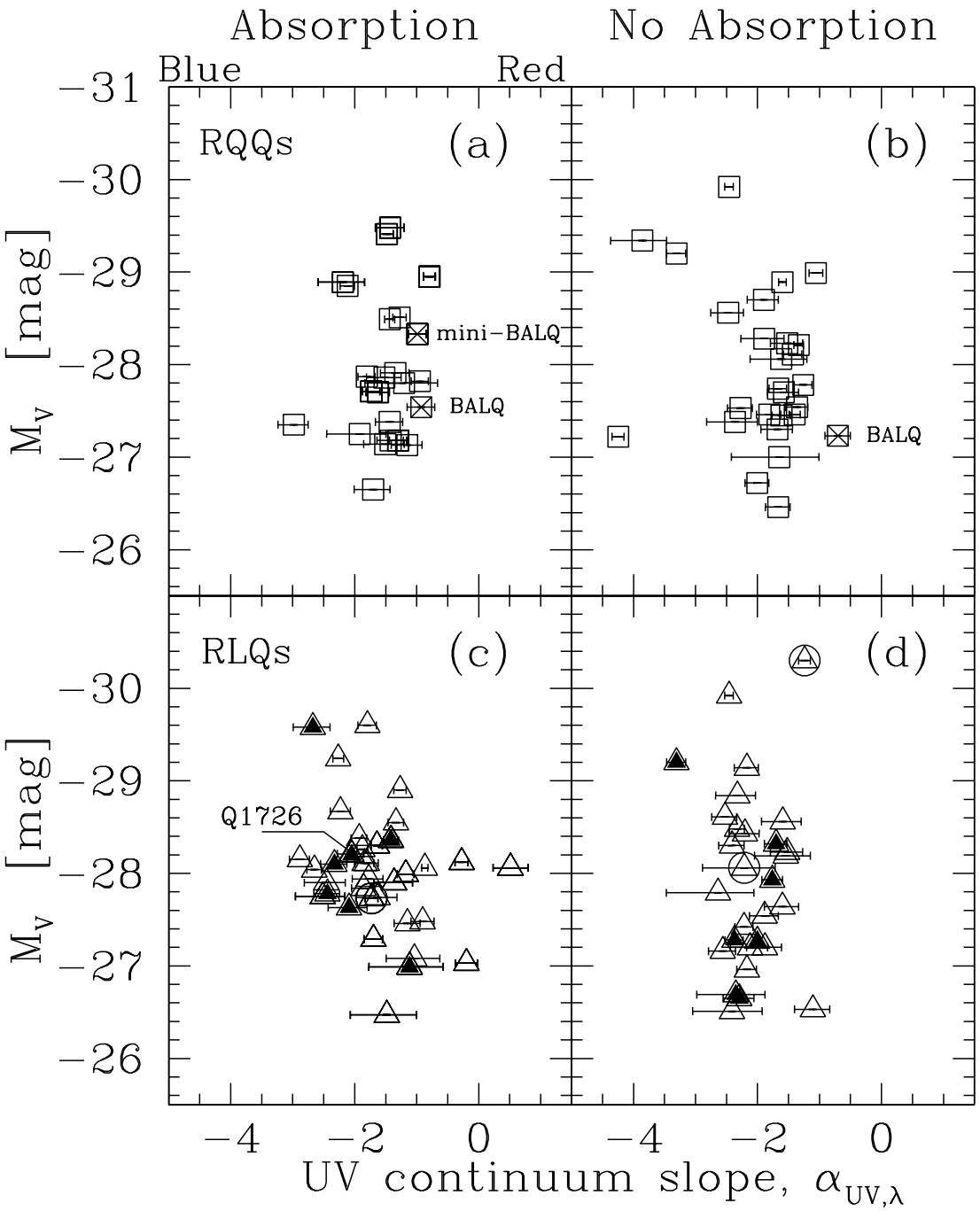

FIG. 2.— Distributions of M_V and $\alpha_{UV,\lambda}$ ($F_\lambda \propto \lambda^{\alpha_\lambda}$) for the quasars [(*a*) and (*c*)] with C IV NALs (triangles: RLQs; squares: RQQs) and [(*b*) and (*d*)] without C IV NALs. The typical uncertainty in M_V is ∼0.5 mag. The RQQs with broad absorption lines (BALs) and mini-BALs (one BAL RQQ has no NALs and is hence plotted in panel b) and the RLQ Q1726+344 with a mini-BAL are marked. The compact steep spectrum (CSS; solid triangles) and giga-hertz peaked radio sources (GPS; encircled triangles) are shown with separate symbols.

a larger dust reddening on average.

The dependence of the total NAL strength ($EW_{\rm tot}$) for each object on source luminosity is different for the two quasar types (Fig. 3b, d; Fig 4); the two luminosity measures, M_V and $L_{\rm cont}(1550\text{Å})$, show consistent results. For RLQs the NALs tend to get weaker in more luminous objects (Figs. 3d and 4b, Table 5). The inverse $EW_{\rm tot} - L_{\rm cont}(1550\text{Å})$ correlation is even more significant ($r = -0.37$ and $P = 0.9\%$) when the individual absorbers are tested (see also Paper I). However, the robustness of this luminosity dependence is unclear because (a) the relationship essentially disappears when the $EW_{\rm tot} < 0.5$Å absorbers are omitted (Fig. 3d, Fig 4, right) and (b) it is not known with certainty that the omitted absorbers (in item (a)) are associated with the quasar (§ 3). More importantly, there is a noticeable lack of $EW_{\rm tot} \geq 0.5$Å absorption in quasars with $M_V \lesssim -29$ mag. This is in sharp contrast to the NALs in RQQs (Figs. 3b and 4a, Table 5):

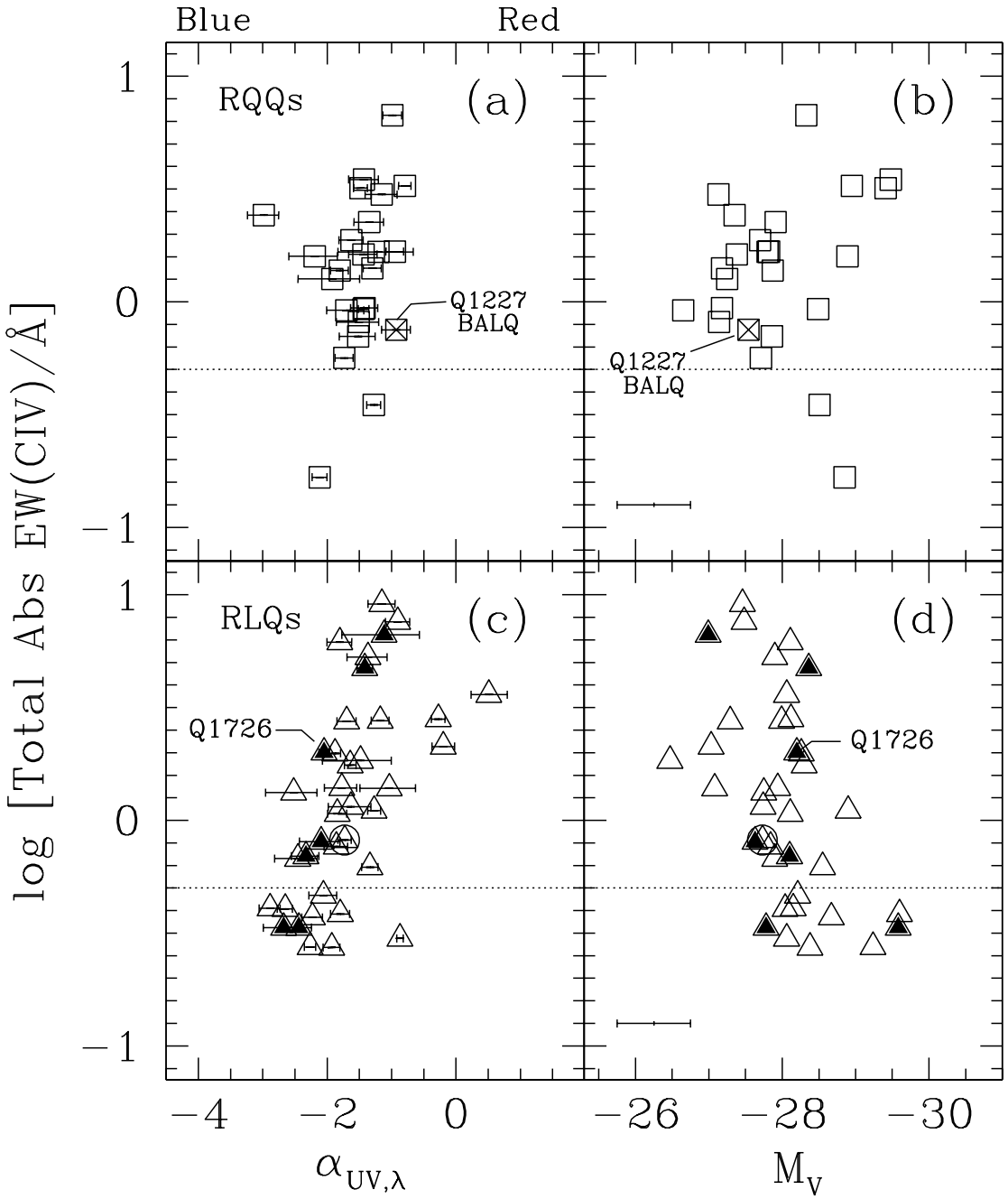

FIG. 3.— Distributions of the total restframe strength of the narrow absorbers (EW) in each quasar relative to (*left*) the UV continuum slope, $\alpha_{UV,\lambda}$, and (*right*) to the quasar luminosity, M_V. The strengths of the narrow absorber detected in the broad absorption line quasar, Q1227+120, and of the RLQ Q1726 mini-BAL are highlighted. Symbols are otherwise as in Figure 2. The dotted lines show the 95% completeness level (0.5Å).

stronger NALs occur in more luminous RQQs. In particular, most of the RQQs in Fig. 3b with $M_V \leq -29$ mag have $EW_{\rm tot} \gtrsim 3$Å. The $EW_{\rm tot}-$ luminosity correlation for the RQQs is significant at the 95% level (Table 5); the NALs of the two RQQs with $EW_{\rm tot} < 0.5$Å are likely intervening. This result is intriguing, if real, because an increasing absorber strength is naively expected if increased radiation pressure in more luminous, bluer objects is responsible for heating the accretion disk and evaporating more absorbing gas off the disk (e.g., Paper I; Laor & Brandt 2002). This is briefly discussed in § 4.5.

There appears to be an upper envelope in $EW_{\rm tot}$ for increasingly redder slope for the RLQs in Figure 3c. This suggests that strong NALs are avoided in very blue objects. The individual subgroups of RLQs (CDQ, LDQ, CSS, GPS) are seen in Figure 4 to distribute fairly similarly within the covered values of luminosity and absorption strength, although the CDQs do not have NALs with $EW \gtrsim$3Å.

The distribution of RQQ NALs in Figure 3a is consistent with that defined by the RLQs in Figure 3c, but the popu-

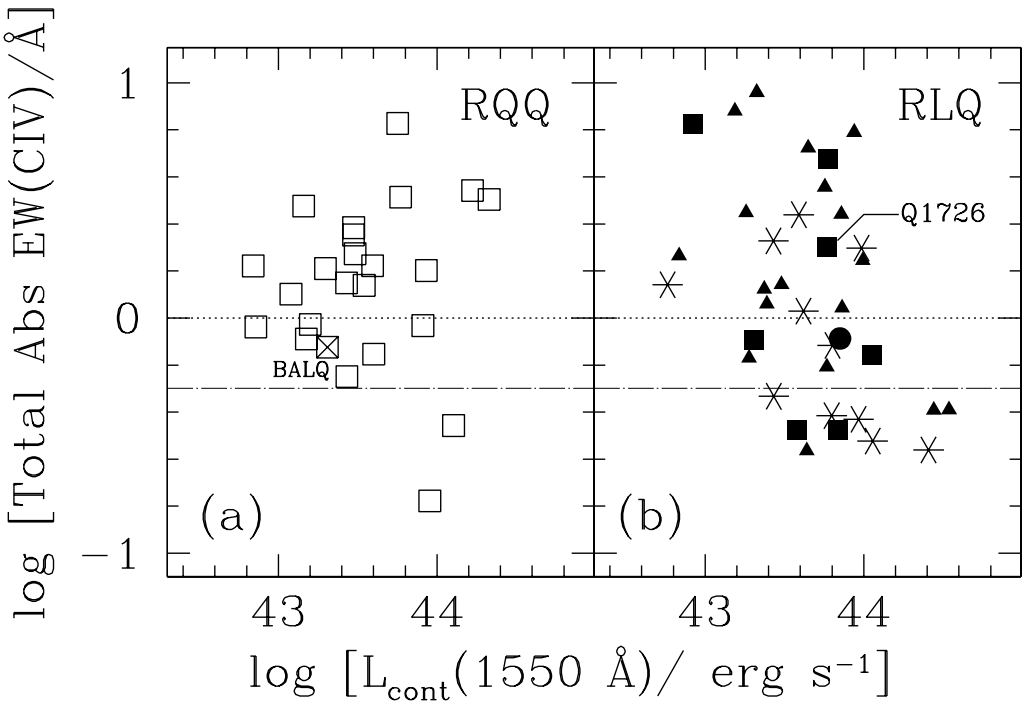

FIG. 4.— Distributions of the total narrow absorber restframe strength, EW, for each quasar with the UV continuum luminosity for (a) the RQQs and (b) the RLQs. Symbols: open squares: RQQs; solid squares: CSS; asterisks: core-dominated quasars (CDQ); small solid triangles: lobe-dominated quasars (LDQs); large solid circle: GPS source. The dotted horizontal line marks the division (EW = 1Å) between weak and strong absorbers adopted in this work. The dot-dashed line shows the 95% completeness level (0.5Å).

lation of weak absorbers in very blue RQQs ($\alpha_{\rm UV,\lambda} < -2.$), as seen for the RLQs, is missing. The single RQQ outlier at $\alpha_{\rm UV,\lambda} \approx -3$ has a low-velocity absorber which also absorbs part of the underlying continuum. This particular system may therefore be located outside the central engine, perhaps even in the quasar host galaxy, along our line of sight. This could explain why this absorber does not follow the trend outlined by the other, mostly intrinsic, absorbers.

4.3. *Dependence on Radio Source Inclination*

Figure 5 shows how the total NAL strength in a subset of the RLQs distribute with the two measures of radio source inclination described in § 2. As discussed in § 4.1, NALs are more frequently occurring in LDQs than CDQs. Figure 5 illustrates that LDQs also tend to be more strongly absorbed than CDQs. This is not a new result (e.g., Anderson et al. 1987; Foltz et al. 1988; Wills et al. 1995; Barthel et al. 1997; Ganguly et al. 2001; cf. Baker et al. 2002 and § 5). LDQs are believed to be intrinsically similar to CDQs, just viewed at a larger inclination, i, of the radio axis relative to our line of sight (§ 2). Hence, absorption strength may, in part, depend on source inclination. Barthel et al. (1997) used almost the same RLQ sample as that currently analyzed. Here, the inclination dependence of the NAL EWs is tested on a more well-suited sub-sample of the RLQs than done by Barthel et al. This is important if the NALs are intrinsic to the quasar central engine and, for example, depend on intrinsic source brightness. Therefore, to avoid possible selection biases the LDQs and CDQs were selected for this particular analysis to cover the same range in the luminosity of the extended radio emission, $L_{\rm ext}$, as illustrated in Figure 6a. The extended emission, as opposed to the compact, nuclear "core" radio emission, is isotropically emitted and is thus a better measure of the intrinsic radio power. Figure 6b confirms that for this subset of RLQs the total NAL strength for each quasar is not correlated with $L_{\rm ext}$, as expected for a sample unbiased in intrinsic radio power. Also, it is comforting that there is no EW dependence on the total radio luminosity, $L_{\rm radio}(5\,{\rm GHz})$, both for the full sample of RLQs (see e.g., Fig. 3 in Paper I) and for the subset (not shown but the distribution is similar to that of the full sample). Figure 5 shows that even for this subsample, the strongest ($EW > 3$Å) NALs are seen in LDQs and the strength increases with[7] inclination (lower $\log R_{\rm 5GHz}$ and $\log R_{\rm V}$); again, this is similar to the full RLQ sample (not shown but see e.g., Fig. 1 by Barthel et al. 1997). The fact that this trend exits in the subsample and the various non-restricted samples of NALs mentioned above shows that the trend is not due to intrinsically brighter or fainter lobe-dominated sources in those samples. If indeed LDQs are relatively more inclined, then the correlations of NAL strength, EW, with $\alpha_{\rm UV}$, $\log R_{\rm 5GHz}$, and $\log R_{\rm V}$ (Figures 3 and 5) can be explained as a combination of inclination and reddening effects, which thus in RLQs seem to dominate possible radiation pressure effects on disk outflows; as argued in § 4.2 a luminosity dependent absorption strength is expected in the latter scenario.

[7] Fig. 4 in Paper I shows this distribution for the strength of the individual absorbers.

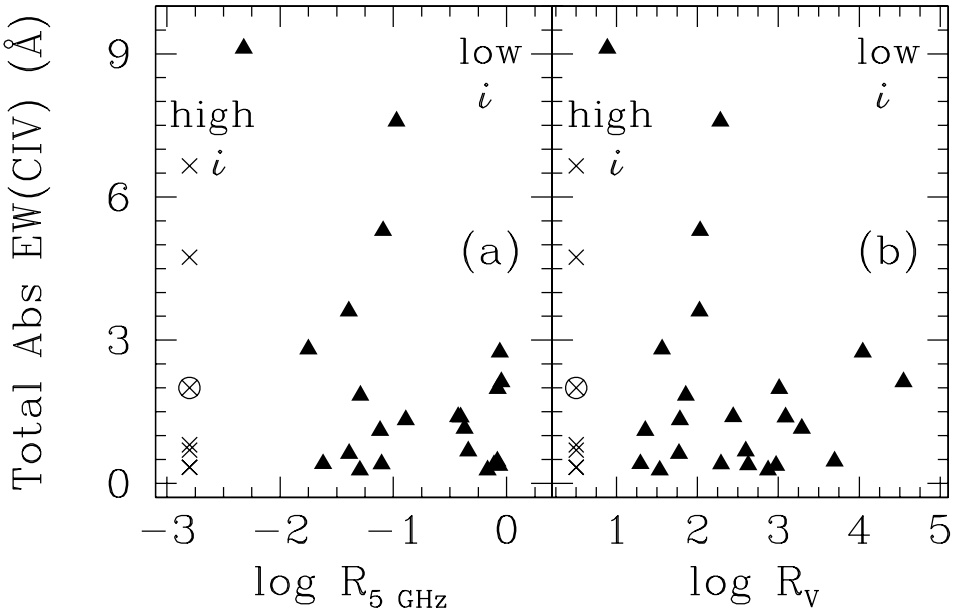

FIG. 5.— The total absorption strength for each RLQ versus estimators of the radio source inclination (i) relative to our line of sight, defined in § 2. Only the subset of RLQs defined by Fig. 6 is shown. Recall, LDQs have $\log R_{5\,\mathrm{GHz}} < -0.3$. The absorption strengths of all the CSS objects in the full sample are shown as crosses at the very left part of each panel. This is because the radio core luminosity is commonly not well determined for CSS quasars, inhibiting an estimate of i. Q1726+344 with a "mini-BAL" trough is encircled.

Such related effects of absorption and reddening are not clearly present for the RQQ sample (Figs. 3 and 4). However, the lack of, even crude, inclination measures for RQQs precludes a sample selection to test inclination dependent absorption strengths. This likely explains the concentration of α_λ in Figure 3a. However, the BAL quasars suggest that a similar inclination dependent distribution of reddening dust exists in RQQs, since (a) the BALs are among the reddest RQQs (§ 4.2), and (b) BAL outflows are likely equatorial (§ 1). Furthermore, it is generally a worry that the optically selected quasars detected in early surveys are biased toward the brightest and hence the least dust reddened sources. This is because sources viewed almost face-on are likely more luminous and bluer, rendering them more easily detected when at large distances. But Figure 3a shows that the current RQQ sample tends to lack

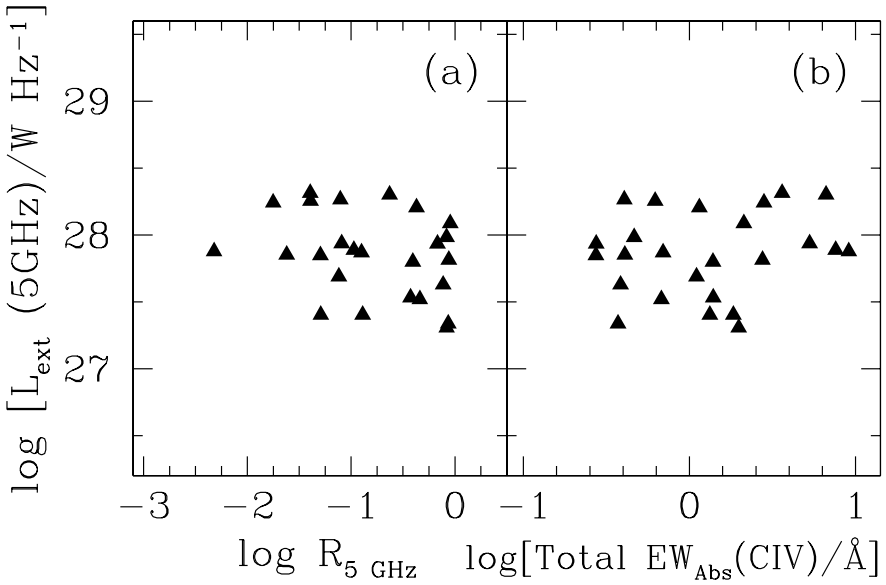

FIG. 6.— Extended radio luminosity shown against (a) the radio source inclination estimator and (b) the total strength of the absorption systems (for each quasar) for the subset of RLQs used in Fig. 5 to test for inclination dependence. There is no bias toward intrinsically brighter/fainter radio sources with inclination angle (panel a). For a given intrinsic source brightness there is a range of absorption strengths (panel b).

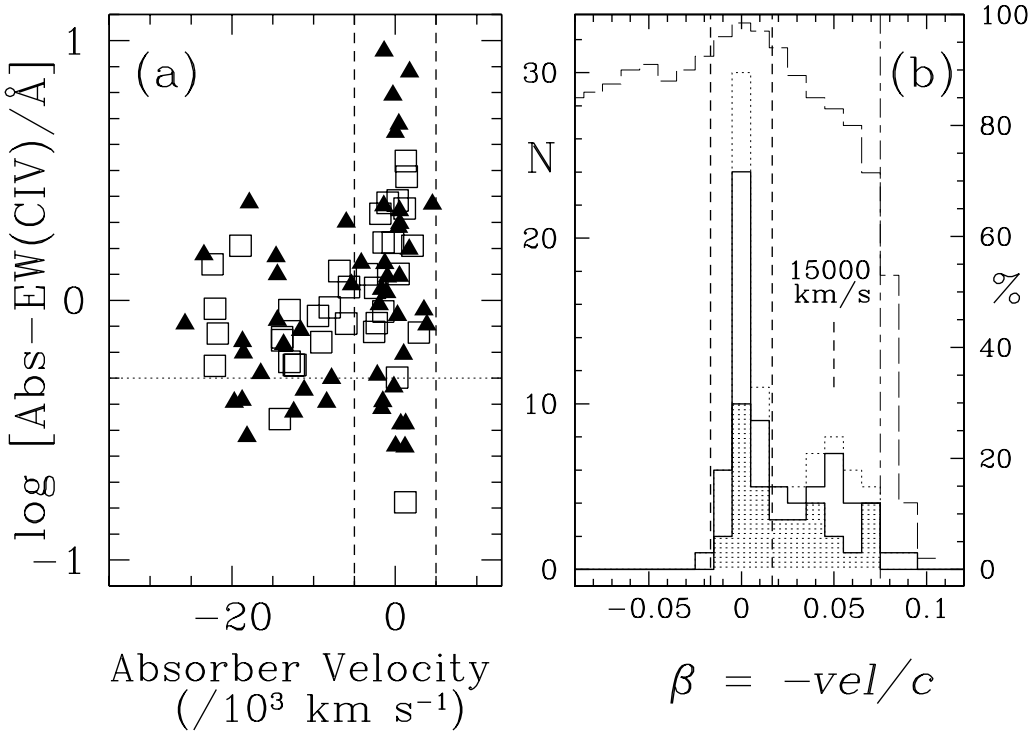

FIG. 7.— (a) Relationship between the strength and velocity of the individual C IV narrow absorber for RQQs (open squares) and RLQs (solid triangles). The velocity space commonly considered for associated absorbers, $|vel| \leq 5000$ km s^{-1}, is marked. The 95% completeness level within $|\beta| \leq 0.02$ (6 000 km s^{-1}) is $EW_{\rm rest} \geq 0.5$Å (Fig. 1). The horizontal dotted line marks this completeness level. (b) Number distribution (left y-axis) of narrow absorber velocity, parameterized as β (defined in the text). The dotted light style histogram represents the distribution with respect to β for the full sample of absorbers among the RLQs and RQQs. The subsample of C IV doublet absorbers stronger than the completeness limit of 0.5Å (rest-EW) are shown by the open solid histogram; the RQQ subset thereof is shown shaded. See Fig. 8 for the RLQ subsets. The range in β consistent with associated absorbers is marked by the two vertical dashed lines. The dashed histogram (right y-axis) shows the completeness level of absorbers down to $EW_{\rm rest} = 0.5$Å for a given β. A completeness level greater than 70% is obtained for $\beta \leq 0.07$ (long/short dashed vertical line).

sources with very blue spectra ($\alpha_{\rm UV,\lambda} < -2$) compared to the RLQs (Fig. 3c). Also, while the most luminous and blue RLQs tend to have weaker NALs and a larger number of them (Figs. 3c and 3d), the RQQs of similar luminosity to the most luminous RLQs tend to have the strongest NALs (compare Figs. 3b and 3d), as noted in § 4.2. Since BAL quasars tend to be relatively redder and less luminous (Brotherton et al. 2001; Goodrich 2001; Hall et al. 2002), to have strong absorption, and are most likely highly inclined (§ 1), could the omission of BAL EWs from Figure 3 explain the lack of a correlation similar to that seen for the RLQs? This is not very likely as BALs are *much* stronger than NALs. For example, the strength of the BAL feature of the one BAL quasar that sneaked into the RQQ sample is ∼27 Å. Inclusion of this BAL in Figure 3b would place it far from the parameter space and trends defined by the NALs at no clear extension of the trend seen in Figure 3a and 3b. However, the BAL strength and M_V of this quasar is consistent with trends defined by low-redshift BAL quasars (Laor & Brandt 2002; Vestergaard 2004b).

4.4. *Velocity Distribution of the Absorbers*

In Figure 7a the EW of each NAL is shown as a function of the absorber velocity relative to the quasar C IV emission redshift. The number distribution of individual $EW \geq 0.5$ Å NALs with velocity (parameterized by β) are shown for the various quasar types in Figures 7b and 8. The commonly adopted velocity limits (± 5000 km s^{-1}) for the associated absorbers (Foltz et al. 1986) are marked. The strongest NALs are clearly *associated* with the quasars (Fig. 7a). Set aside the five strongest NALs in RLQs, there is a similar velocity distribution for RLQs and RQQs. The enhancement of associated NALs is evident and quantified in Figure 7b. A second peak is present at a velocity of $-15\,000$ km s^{-1} (see also Fig. 7a). The RQQs contribute significantly to this enhancement by having a large number of absorbers over a range of outflow velocities. The RLQs are characteristically strongly clustered around $-15\,000$ km s^{-1} (Fig. 8) with LDQs contributing the most. This clustering around $\beta \approx 0.05$ roughly coincides with the increase in absorber strength (Fig. 7a) at a velocity around $-18\,000$ km s^{-1}. Notably, this EW increase is present for both RLQs and RQQs.

The long-dashed histogram in Figures 7b and 8 shows the completeness level of NALs down to $EW_{\rm rest} = 0.5$Å for a given β bin. The high completeness fraction ($> 70\%$) across the entire second enhancement (both in EW and β parameter space) shows that these enhancements are real. While there is a danger that the weaker NALs ($EW < 1$Å) at high velocity may be unidentified intervening systems, more so for the RQQs (§ 3), there is little doubt that the stronger ($\gtrsim 1$ Å), high-velocity absorbers are intrinsic to the quasars (see Figure 7a).

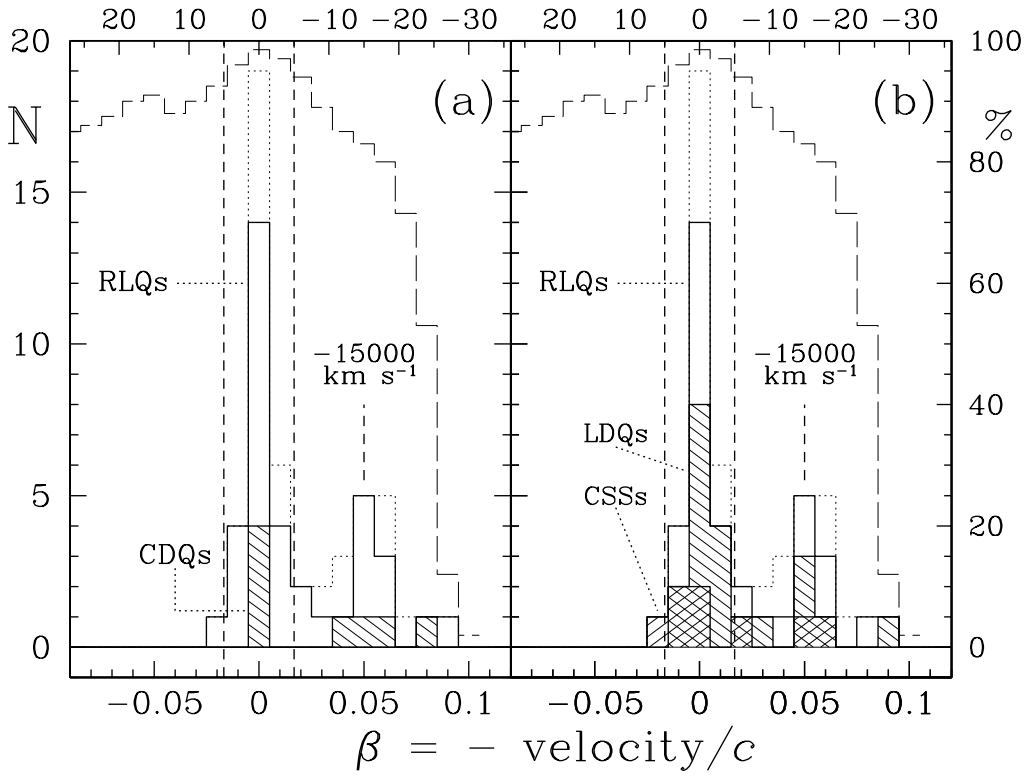

FIG. 8.— Number distributions (left y-axis) of the β parameter of the narrow absorbers detected in the RLQs and various radio quasar subsets, as marked. The absorber velocity is shown in the top x-axis in units of 1000 km s^{-1}. Only absorbers stronger than the 95% completeness limit within $|\beta| \leq 0.02$ of 0.5Å rest-EW are included here (solid histograms; dotted histogram: full sample of RLQ absorbers). The dashed histogram (right y-axis) shows the completeness level of absorbers down to $EW_{\rm rest} = 0.5$Å as a function of β.

4.5. *Are NALs Related to Quasar Outflows?*

The more dramatic BALs are due to large column densities of outflowing, absorbing gas (e.g., Hamann 2000). The quasar-intrinsic NALs may also be associated with outflowing gas somehow, since (i) strong (i.e., likely quasar intrinsic) high-velocity NALs exists, and (ii) the high-velocity enhancements at $v \approx 15\,000 - 18\,000$ km s^{-1}, discussed above, are intriguingly close to the typical BAL terminal[8] outflow velocity ($\sim$20 000 km s^{-1}). Also, the occurrence and properties of NALs and BALs in RLQs and RQQs are generally consistent with predictions of the disk-wind outflow model of Murray & Chiang (1995). Specifically, RQQs tend to have NALs of modest strength (§ 3.3; Fig. 1a; Fig 7a) and, until recently, were the only quasars known to have BAL systems. Also, RLQs have quite strong associated NALs (§ 4.2), but rarely[9] develop the strong BAL systems (e.g., Goodrich 2001; but see Becker et al. 2001). In the disk-wind model of Murray & Chiang (1995), the stronger X-ray flux in RLQs reduces the radiation pressure on the disk winds by stripping the atoms off electrons. In effect, RLQs are incapable of accelerating the high-density outflows to relativistic velocities and strong, low-velocity absorption is predominantly expected instead. This provides a reasonable explanation for the relative strengths of the associated, narrow absorbers among RLQs and RQQs seen here. In this case, there is an immediate connection between NALs and BALs as the RLQ associated NALs are "failed" BAL systems. (Other, related scenarios were suggested by Elvis 2000; Ganguly et al. 2001; Laor & Brandt 2002).

The moderately strong, high-velocity absorbers seen at velocities close to the BAL terminal velocities add an interesting twist to this interpretation. Since these high-velocity NALs occur in both RLQs and RQQs, they may originate in a second, perhaps different, population of narrow absorbers common to quasars irrespective of radio type. Figure 4 in Paper I shows that these high-velocity absorbers are not confined to objects at a specific source inclination; Figure 8 also shows a mix of CDQs and LDQs with high-velocity NALs.

To explain the presence of high-velocity (associated) NALs in both RLQs and RQQs, two scenarios appear possible: entrainment by BAL outflows or by radio outflows, as discussed in turn next. First, while one may imagine the high-velocity RQQ NALs, typically with $EW \lesssim 3$Å, originate in discrete, turbulent clouds of relatively lower col-

[8] Outflow velocities up to $\sim$60 000 km s^{-1} have, however, been detected (e.g., Jannuzi et al. 1996; Hamann et al. 1997).

[9] Although Becker et al. (2001) find $\sim$10% BALs quasars among bona-fide RLQs (i.e., the radio-loudness, $R^* = L_{\rm radio}/L_{\rm optical} > 10$) almost similar to the RQQ fraction ($\sim$10% − 15%; e.g., Hewett & Foltz 2003), most of the detected BAL quasars are radio-intermediate sources ($1 \leq R^* \leq 10$); the radio-intermediate nature appears common among BAL quasars in general (Francis, Hooper, & Impey 1993) often owing to the absorption and reddening of the optical emission (e.g., Goodrich 2001; Becker et al. 2001). The relative distribution among radio type is unknown at present, but since many are highly absorbed (see Hall et al. 2002 for unusually looking BAL quasar spectra from Sloan Digital Sky Survey), and apparently radio-intermediate, most of the BAL quasars are presumably intrinsically radio-quiet.

umn density gas entrained by the BAL outflow, this cannot easily explain the high-velocity absorbers in RLQs: BAL outflows are rarer and some shielding from the fatal X-ray flux would seem necessary to allow radiation pressure acceleration of these NAL systems. Besides, BAL outflows are *not* detected in these RLQs with high-velocity NALs. Alternatively, these high-velocity absorbers may originate in gas stirred up and perhaps entrained by the radio jet. However, such a scenario appears a little contrived given the similar occurrence in RQQs, unless these RQQs in fact have some weak radio source outflow which could possibly entrain NAL gas. To test this, the NED[10] radio data base was searched for indications that the two RQQs with strong ($EW > 1$Å) high-velocity NALs (Figure 7a) are radio sources. Neither of the FIRST nor NRAO VLA Sky Survey 1.4 GHz radio images reveal any radio emission down to 1 mJy within ∼1 arcminute of the optical position of the RQQs. Deeper radio imaging at lower frequency is needed to determine whether these RQQs may have some weak, uncollimated radio outflows which could possibly account for accelerating the intrinsic NAL absorbers. Instead, Ganguly et al. (2001) propose that RQQs have higher mass-loss rate, a higher wind velocity, and in effect have winds with higher matter densities compared to RLQs. While this may explain the dearth of BALs in RLQs, it does not explain the intermediate and weak NALs ($EW_{\rm rest} \lesssim 3$Å) at high outflow velocities seen for both RQQs and RLQs. Also, Vestergaard (2004b) finds no support for RQQs typically having higher $\dot{M}_{\rm BH}/\dot{M}_{\rm Edd}$ than RLQs in this $z \approx 2$ quasar sample.

In summary, the presence of strong associated NALs in RLQs and the presence of relatively weaker associated NALs in RQQs are quantitatively consistent with expectations of radiatively driven disk-wind scenarios. The ∼1Å high-velocity NALs may originate in a second population of narrow absorbers. Entrainment by either BAL outflows or radio plasma outflow do not appear to uniquely and easily explain their presence in both RLQs and RQQs.

5. IS ABSORPTION RELATED TO RADIO SOURCE EVOLUTION?

One subset of the RLQs, the CSSs, may be able to shed light on whether absorption in RLQs is related to the onset and propagation of the radio source (Baker et al. 2002). The reason is that CSSs are possibly[11] young (O'Dea 1998) and, as can be seen in Figure 5, CSS absorbers exhibit a range of strengths and some are relatively strong. Baker et al. (2002) propose that associated NALs in CSSs are in fact related to the radio source evolution, based on their study of C IV λ1549 associated absorbers for RLQs at $0.7 < z < 1.0$ and $1.5 < z < 3.0$ detected in the well-defined Molonglo radio survey (Kapahi et al. 1998). The original low-frequency (408 MHz) selection and high completeness level (∼97%) down to the survey limit of 0.95 Jy in a well-defined area on the sky make the Molonglo radio survey one of the least biased surveys with respect to radio source inclination, i (Baker et al. 2002). Baker et al. find that the most strongly absorbed objects ($\lesssim$ 5Å) in their sample are both the most dust reddened and have the smallest radio sources, most of which are CSS in nature. While Baker et al. do find their LDQs to be more strongly absorbed than their CDQs (similar to earlier findings and this study; see § 4.3), the CSS quasars are after all the most strongly absorbed. The authors propose to see an effect of radio source evolution in which the young radio source is enshrouded in gas and dust: at early radio source age the nuclear spectrum is seen through a large amount of reddening dust and absorbing gas. But with time, as the radio source grows, this cocoon is shed and dispersed or destroyed leaving less material (or covering fraction thereof) to absorb the centrally emitted spectrum.

Curiously, the inverse trend between linear radio source size and absorber strength seen by Baker et al. is in sharp contrast to the data studied here. Figure 9 shows how the total associated-absorption strength for each RLQ distributes with the 'largest linear radio source size' (Miley 1971); the completely opposite trend is evident. The CSS quasars show a range of absorption strengths, some of which in fact have high outflow velocities (Figure 9b). The GPS and CSS phenomena are possibly related (e.g., O'Dea 1998) and the one absorbed GPS object also has a high velocity, but relatively weak, absorber. Although two of the CSSs have similar or stronger absorption than the CSS objects in the Baker et al. (2002) sample, the LDQs with large radio sources after all have the strongest associated NALs. In fact, there appears to be a lower envelope in the linear size for a given absorber EW for the current sample. Furthermore, there is no apparent relation between absorber velocity and linear radio size for this sample (Figure 9b).

In an attempt to better understand the discrepant results with the Baker et al. study, the properties of the two RLQ samples have been compared; the focus was placed on the high redshift ($1.5 \leq z \leq 3.0$) subset of the Baker et al. quasars which has similar redshift range to the current RLQ sample. An important issue is that of sample selection. Most of the RLQs studied here were originally detected in low-frequency (178 MHz and 408 MHz) surveys (§ 3) similar to the Molonglo quasars. Also, while the RLQ sample studied here is non-homogeneous and incomplete, this nature is both a liability and an asset. The sample does have the advantage that it is selected to reduce selection biases. For example: (a) the most beamed sources are not included, (b) RLQs with a range of source inclinations were selected (§ 3), and (c) some control over the intrinsic brightness is employed (§ 3 and § 4.3). However, these RLQs are also expected to be more luminous than the Molonglo sources, owing in part to their original detection in earlier surveys that were less sensitive than more recent surveys commonly are, and this also appears to be the strongest difference between the two samples. A comparison based on M_V and 408 MHz radio luminosities, L_ν(408MHz), confirms this (Table 6): this RLQ sample is more luminous on average by ∼1 dex in L_ν(408MHz) with very little overlap with the Baker et al. values, and by 1.5 magnitude in M_V. In summary,

[10] NASA/IPAC Extragalactic Database

[11] The alternative interpretation is that a very dense intergalactic medium confines the radio source to a very small physical size, preventing significant radio source growth ("frustrated radio source"). However, the data currently appear to favor the young source interpretation (see O'Dea 1998 for a review).

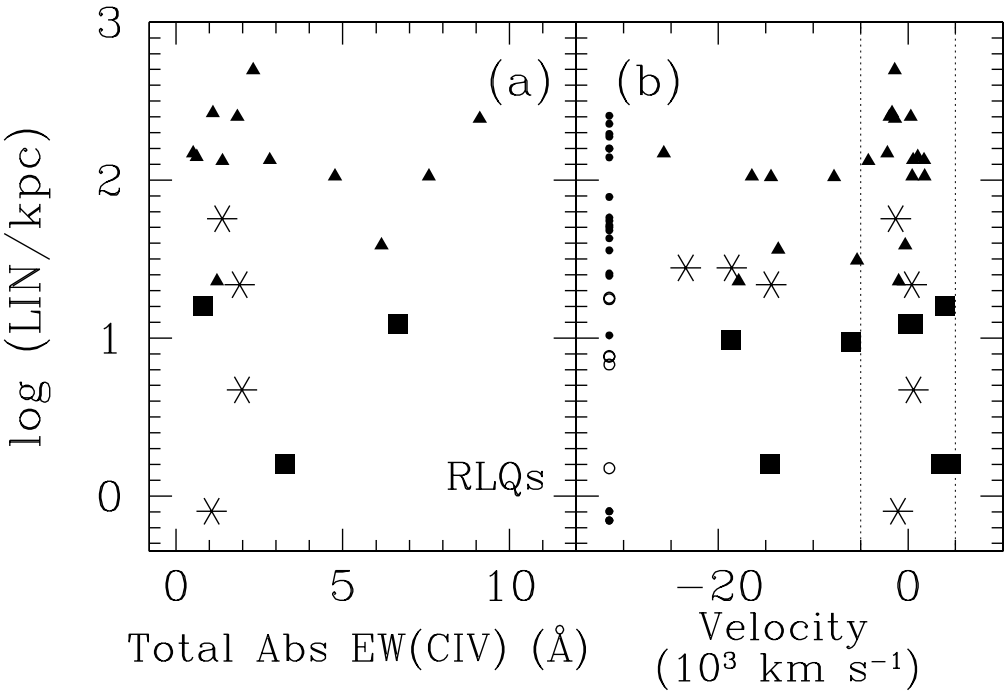

FIG. 9.— Linear radio source size shown relative to (*a*) total absorption strength for each RLQ and relative to (*b*) the individual absorber velocity. Only absorbers stronger than the 95% completeness limit within $|\beta| \leq 0.02$ of 0.5Å rest-*EW* are included here (both panels). In addition, only *associated* absorbers are included in panel (a) to ease a direct comparison with Baker et al. (2002). (The absorbers omitted from that panel mostly occupy the region below LIN of 100 kpc and $EW \lesssim 2$Å.) Note that the use of the total *EW* for each quasar is appropriate for assessing which quasars are more strongly absorbed and is fully comparable to the Baker et al. study. The distribution of linear sizes of unabsorbed RLQs (open circles: CSS; solid circles: other RLQs) are shown at a relative velocity of $-30\,000$ km s^{-1} for reference. Symbols: solid squares: CSS; solid triangles: LDQs; asterisks: CDQs. Note: to aid a direct comparison with Baker et al. (2002), $H_0 = 50$ km s^{-1}Mpc^{-1}, $q_0 = 0.5$, and $\Lambda = 0$ is adopted for the linear sizes, which are $\simeq 0.61\times$ LIN(H_0=50;q_0=0.0).

the Molonglo quasars are intrinsically fainter (radio and optical) sources. Also, they have a higher fraction of CSS quasars (11/20) compared to this RLQ sample (14/66; Table 3). Hence, the Molonglo sample contains a larger fraction of young sources, if the Baker et al. scenario holds.

Assuming low-frequency selected, weaker radio sources are typically younger[12], can radio source age explain the different absorption characteristics seen in these two studies, such that the current RLQs are relatively older? In that case, the Molonglo quasars should (1) be more frequently absorbed, (2) be more strongly absorbed, and (3) be dust reddened to a higher degree. The Baker et al. $1.5 \leq z \leq 3.0$ sample not only has a higher fraction of CSS quasars with associated NALs (8/11 $\simeq$73% $\pm$25%), but the quasars are also more frequently absorbed in general (18/20 $\simeq$ 90%$\pm$21%); in comparison, only 36% $\pm$ 16% of the CSSs and 39% $\pm$ 8% of the RLQs here have associated NALs, even when counting all the detected NALs (these fractions are not shown in Table 3) as opposed to the most complete subset ($EW \geq 0.5$Å; § 3.3). However, the occurrence of CSS NALs are marginally consistent between the samples to within the (large) counting errors. On the strength of the NALs, the Molonglo quasars are generally *less* strongly absorbed: none of the Baker et al. non-CSS quasars display absorption stronger than 2Å, while many of the LDQs and CDQs studied here are more strongly absorbed. However, the NAL strength of the CSS quasars is comparable between the two samples (e.g., compare Figure 5 [$EW \lesssim 7$Å] with Figure 7 by Baker et al. [$EW \lesssim 5$Å]). Regarding the degree of dust reddening, as judged from the UV continuum slope (α_λ) the Molonglo quasars are not subject to a significantly higher dust column than the current RLQs: the range of α_λ measured among the absorbed RLQs is relatively similar between the two studies. Specifically, the absorbed Molonglo quasars cover the approximate range $-2 < \alpha_\lambda < 1$, which overlaps with most of the spectral slopes measured here for the RLQs (Figure 3; note that also the CSSs display a range of slopes). However, the trend between reddening and absorption strength in the Baker et al. sample is fully consistent with the data presented here. Since the RLQs in this study also tend to be more strongly absorbed, radio source evolution do not appear to explain the differences seen with the Baker et al. study. This is supported by the model-predicted (Begelman 1999) and observed (e.g., O'Dea 1998) negative luminosity evolution with radio source growth. Hence, other effects must be at play and dominate possible radio source age differences

[12] How may low-frequency surveys be more sensitive to relatively younger radio sources? Presumably, a young source with poorly collimated radio outflow will emit predominantly isotropic, steep spectrum radio emission. We may be seeing this already for the (very faint) radio-sources in RQQs (e.g., Barvainis, Lonsdale, & Antonucci 1995; Kukula et al. 1998). Likewise, a source in which the infant radio jet is so small that it contributes negligibly to the overall radio power would also tend to emit mostly isotropic lobe emission. In both cases these steep spectrum sources are most easily detected in low-frequency surveys.

between the samples.

An alternative possibility is that the deviating results are due to a statistical fluke in either or both studies as the results are after all based on small number statistics: in regard to NALs with EW >3Å the Baker et al. sample has six NALs of which two are detected in $z > 1.5$ CSSs with EWs larger than that of a single $z > 1.5$ LDQ narrow associated absorber with $EW > 3$Å (Figure 8 by Baker et al.). In comparison, this RLQ sample has six NALs, two of which are observed in LDQs with EWs larger than that of the two CSS NALs (Figure 9).

In summary, both RLQ samples exhibit stronger absorption in more dust reddened objects, but the current sample does not support the findings of Baker et al. that CSS quasars are the most strongly absorbed sources. Also, it does not appear likely that radio source evolution explains the different absorption properties between the samples as expected if the RLQs studied here are the more aged cousins of the presumably young radio sources detected in the low-frequency Molonglo survey. Rejecting the possibility that the differences are due to a statistical fluke, one is left to conclude that luminosity differences and sample selection most likely are the leading causes of the differing results obtained. The reason is that the RLQs in this work are on average more luminous in the radio by about a factor 10 and in the optical by about a factor 3 (Table 6) than the Baker et al. sample. The higher luminosities may somehow make the current RLQs more capable of producing stronger absorption. This issue is addressed by Vestergaard (2004b).

5.1. *Speculations*

5.1.1. *Luminosity Driven Absorption?*

How may a higher source luminosity of the RLQs in this study explain their stronger absorption relative to the Molonglo quasars? More luminous sources may subject the accretion disk and the immediate environment of the central engine (including a 'torus', if present) to a larger radiation pressure which could generate and accelerate larger amounts of absorbing material (e.g., Proga et al. 2000; Laor & Brandt 2002). While the properties of the absorbed RLQs in this study seem to show that radiation pressure effects do not dominate over inclination dependent distributions of reddening and absorbing material, the RQQ NALs after all do support the radiation pressure interpretation (§ 4.2, § 4.3). Hence, one may speculate that the luminosity dependent absorption trend (allegedly caused by radiation pressure-driven, absorbing disk outflows) is only visible for RLQs across several orders of magnitude in luminosity, as opposed to the relatively narrow ranges ($\lesssim$1 dex) studied here and by Baker et al. (2002). Alternatively, the strong, associated NALs detected in the more luminous, larger scale radio quasars may be of a different origin than the CSS absorbers.

However, an investigation based on well-selected quasar samples specifically targeted to address these issues are required to disentangle the effects of radio source age from effects owing to the mass, luminosity, size, and/or inclination of the source, in addition to the complicating effects of merger history and star formation on the amounts of matter available for reddening and absorption. It is hoped that these intriguing differences discussed above will motivate further studies of these issues, because an understanding of the evolution of active nuclei and quasars is important for our understanding of many other phenomena, including star formation and galaxy evolution.

5.1.2. *Are Young CSS and BAL Quasars Connected?*

On a slightly different but relevant note, it is interesting to speculate that the recently discovered high-ionization BAL quasars among the 1.4 GHz selected FIRST sources (Becker et al. 2001) are in fact CSS quasars, even if most are radio-intermediate and not bona-fide RLQs. The reason is that BAL quasars display compact, often unresolved, radio structure, yet they essentially all have steep radio spectra. In addition, for low-ionization BALs there is evidence that the BAL outflow phenomenon is connected with a recent merger and/or starburst in the host galaxy (Canalizo & Stockton 2002), which may also trigger a radio source (Baker et al. 2002). While this is much harder to establish for the more distant high-ionization BALs, it is indeed an intriguing possibility. The radio-loud, high-ionization BAL quasar, FIRST J1556+3517, may be the first known example (Najita et al. 2000). This interpretation is, however, not immediately consistent with the lack of BAL quasars in the Molonglo survey, unless the RLQ BAL phase is very short.

5.1.3. *On the Possible NAL Connection with Radio Source Evolution*

If the onset of nuclear activity simultaneously triggers the radio source and an initial BAL phase as suggested above, then at least the dynamical time-scales for these outflows should be consistent. For the radio-quasar 3C 191 (Q0802+103), with a strong (∼7Å) associated NAL in its spectrum, the available data allow a crude test thereof. Indeed, dynamical time-scale estimates suggest that 3C 191 could have started its nuclear activity expelling a BAL wind (or a birth cocoon) that is now observed as a distant, slow-moving NAL wind. Specifically, this requires (a) that the low-velocity ($v \lesssim 1400\,\mathrm{km\,s^{-1}}$) absorbing gas started out as a high-velocity BAL outflow ($v \gtrsim 20\,000\,\mathrm{km\,s^{-1}}$) that later decelerated significantly before reaching its current location ∼28 kpc from the central engine (Hamann et al. 2001), (b) that the radio source expanded[13] with a constant speed of $\sim 0.02c$ (Readhead et al. 1996) to its current linear size of ∼40 kpc (Lonsdale et al. 1993), and (c) that the optical-to-X-ray slope, $\alpha_{\rm OX}$, was much steeper at early epochs, such that this slope flattened as the quasar evolved. This is because BAL quasars typically have steeper slopes $\alpha_{\rm OX} \gtrsim 2$ (Brandt et al. 2000; Green et al. 2001) than that observed for 3C 191 (∼1.4; Wilkes et al. 1994). Also, flat $\alpha_{\rm OX}$ are not conducive to generating high-velocity BAL outflows according to the radiatively driven disk-wind model of Murray & Chiang (1995). In addition, Hamann et al. (2001) argue that the outflow

[13] Radio lobe advancement speeds are never larger than $0.1c$ (Longair & Riley 1979). Hot spot advancement speeds for compact steep spectrum sources are about and not much higher than $\sim 0.02c$ (Readhead et al. 1996). Since these compact, likely young, sources are not located in an environment particularly different from other radio sources (e.g., O'Dea 1998), these expansion speeds should be representative. For example, the advancement velocity of the radio lobes in Cygnus A is comparable (Readhead et al. 1996).

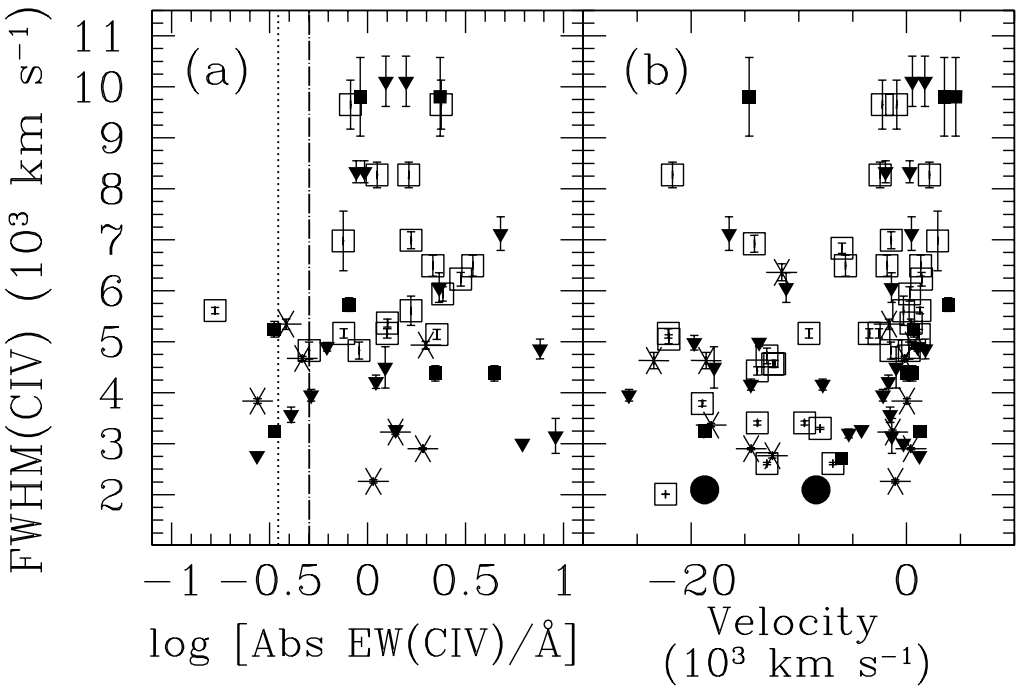

FIG. 10.— Distribution of C IV (*a*) individual narrow *associated* absorption strengths (i.e., $|v| \leq 5000\,\mathrm{km\ s^{-1}}$) and (*b*) individual absorber velocity ($= -\beta c$) with the C IV emission line width of the quasars. The lower detection limit of 0.35Å for CDQs with FWHM(C IV) $< 6000\,\mathrm{km\,s^{-1}}$, as determined by Ganguly et al. (2001), is marked by the dotted vertical line. The detection limit of 0.5Å as determined for the current quasar sample is marked with the dot-dashed vertical line. Symbols: open squares: RQQs; solid triangles: LDQs; asterisks: CDQs; small solid squares: CSS; solid large circles: GPS.

must have swept up some galactic material, since its current mass exceeds that expected for BAL outflows. Interestingly, these authors find their estimates of the size, mass, and velocities of the NAL gas in 3C 191 to be consistent with the inferred values of these quantities for galactic superwinds in low-z starburst galaxies. Alternative scenarios to explain the 3C 191 absorber are discussed by Hamann et al. (2001).

It is currently unknown whether the steep $\alpha_{\rm OX}$ in BAL quasars (a) is an intrinsic property of quasars capable of generating BAL outflows, as predicted by disk-wind models, or (b) is caused by the absorbing mass outflow itself (e.g., Brandt et al. 2000). In the latter case, the nature of the outflow will need to change with time to explain the flat $\alpha_{\rm OX}$ currently observed for the above scenario to be viable.

6. EMISSION LINE WIDTH DEPENDENT ABSORPTION?

Ganguly et al. (2001) find a significant lack of associated absorbers among CDQs with C IV emission line width (FWHM(C IV)) less than $6000\,\mathrm{km\,s^{-1}}$ for the 15 quasars with C IV NALs from their *HST*-observed sample of 59 sources at $z \leq 1$. This observation can be explained if the gaseous region, responsible for the associated NALs, is located away from the radio jet axis (see Ganguly et al. 2001 for details). In that case, our line of sight will not intercept the region occupied by the NAL systems for these sources, since CDQs are viewed at relatively smaller angles to the radio jets (§ 2). It is important for our understanding of the central engine and its evolution to know if such a trend is seen for more distant quasars as well. Table 7 lists for different subsamples the number of absorbed quasars with FWHM(C IV) smaller or larger than $6000\,\mathrm{km\,s^{-1}}$, respectively. These subgroups are further subdivided based on the absorber velocity. For reference, Table 8 gives the distribution of narrow-lined and broad-lined quasars among the absorbed and non-absorbed quasars. Note that in both tables only quasars with NALs stronger than 0.5Å are counted, since this is the most complete subset of NALs. Figure 10 shows how the strength and the velocity of the associated NALs distribute with FWHM(C IV) of the quasars.

Table 7 shows the striking result that for all subsamples − CDQs included − and for all absorber velocities the quasars with relatively "narrow" C IV emission lines (cols. 4 and 7) are *more* frequently absorbed than broader-lined quasars (cols. 3 and 6), in stark contrast to the results of Ganguly et al. In fact, the most strongly absorbed quasars have FWHM(C IV) $\lesssim 5000\,\mathrm{km\,s^{-1}}$ (Figure 10a), and all CDQs with associated NALs ($EW \geq 0.5$Å) are "narrow-lined". After all, the broad-lined and narrow-lined CDQs are equally frequently absorbed (∼33%; Table 8, cols. 6 and 7). But when all detected NALs are taken into account, as many as ∼2/3 of the narrow-lined CDQs are absorbed. In addition, Table 8 shows that with a lower EW cutoff at 0.5Å: (a) narrow-lined quasars are more frequently *unabsorbed* among all the subsamples (cf. col. 4 and col. 6), (b) the RQQs display an even cut (∼40% within the errors) of absorbed objects with low and high FWHM(C IV) (cols. 6 and 7), and (c) broad-lined RLQs as a group are more frequently absorbed, owing mostly to the fact that all the broad-lined LDQs and CSSs are ab-

sorbed; however, care should be taken as the broad-lined RLQ subgroups have large uncertainties. Also, objects with different FWHM(C IV) exhibit no significant differences in absorption strength (Figure 10) with the exception that objects with very broad emission lines lack weak absorbers, $EW \lesssim 0.6$Å (Figure 10a). The CDQs tend to have FWHM(C IV) $< 7000\,\mathrm{km\,s^{-1}}$ but also have NALs with EW up to $\sim$2Å.

In conclusion, the quasar sample here does not support the result of Ganguly et al. (2001) that associated NALs avoid narrow-lined CDQs, although narrow-lined quasars are slightly less absorbed, in general. Specifically, the narrow-lined CDQs with associated NALs are more frequently absorbed than the broad-lined CDQs, a property that all the quasar subtypes share. This conclusion does not change if all detected absorbers are analyzed.

The obvious possible explanations for the different results of our studies are: (a) a luminosity effect in the Ganguly et al. sample causing an absorber cutoff for sufficiently luminous quasars, similar to that seen in Figure 3d, and (b) different sample selections. Although there is an indication that NALs stronger than $EW \gtrsim 0.5$Å are avoided in the most luminous ($M_V < -27$ mag) Ganguly et al. quasars, it is unclear, and at most tentative, whether or not the luminosity effect mentioned in (a) is present. The reason is that the Ganguly et al. NALs are few and exhibit a large distribution in the $EW - M_V$ plane[14] with no distinct correlation. More importantly, the three absorbed flat-spectrum quasars ($\simeq$ CDQs) do not have distinct M_V values from their unabsorbed siblings. In terms of sample selection, the current sample is slightly more optically luminous than the Ganguly et al. quasars (Table 6), which may suggest that low-z quasars are subject to lower amounts and/or different distributions of absorbing gas compared to the distant and more luminous quasars, as also noted by Ganguly et al. (2001). However, sample selection is likely a significant factor considering the fact that the low-redshift BQS quasars display a high absorption frequency and have NAL strengths (Laor & Brandt 2002) similar to those reported here.

7. SUMMARY AND CONCLUSIONS

Weak and strong absorption is relatively common among low-redshift active galaxies, but the fraction of quasars with associated narrow-line absorption is still poorly known, especially at moderate to high redshift. The basic statistics of narrow C IV λ1549 absorption lines detected in moderate redshift ($1.5 \lesssim z \lesssim 3.5$) radio-loud and radio-quiet quasars are presented here (Tables 3 and 4). This sample is particularly suitable for this study for several reasons: (1) it was *not* selected on account of the presence of absorption in the restframe UV spectra, (2) the radio-loud quasars have a large range in radio source inclinations and a significant subset thereof can be defined where intrinsic brightness does not bias inclination dependency tests, and (3) the radio-loud and radio-quiet quasars were selected to match well in redshift and luminosity, minimizing biases in the study due to these two parameters and allowing a fair comparison of the absorption properties of the two radio types. It is important to note that this sample is not complete which may affect the absolute absorption frequencies. However, given the sample selection and the current lack of such statistics, the absorption frequencies should provide fair guidelines until complete samples are analyzed. The main conclusions can be summarized as follows:

(1) Moderate redshift quasars display a high frequency ($\gtrsim$ 52% $\pm$7%) of narrow C IVλ1549 absorption lines (NALs), similar to Seyfert 1 galaxies at low redshift and slightly higher than currently observed for the Bright Quasar Survey (BQS) quasars at $z \lesssim 0.5$. The strength of the narrow absorbers is comparable to those detected in the BQS sample. When restricted to the most complete subset of absorbers ($EW \geq$0.5Å; completeness level $\gtrsim$95%) about 40% ($\pm$ $\sim$9%) of the quasars are absorbed, irrespective of radio type (i.e., including radio-quiet, radio-loud, radio core-dominated, radio lobe-dominated, and compact steep-spectrum sources).

(2) Strong narrow absorbers with $EW_{\rm rest} \gtrsim 1$ Å are detected in $\sim$35% ($\pm$5%) of the quasars with a slightly lower frequency among radio-quiet quasars ($\sim$30% $\pm$8%) compared to radio-loud quasars ($\sim$40% $\pm$8%). However, a constant $\sim$25% ($\pm$5%) of the quasars, irrespective of radio type have strong *associated* absorption (velocity, $|v| \lesssim 5000\,\mathrm{km\,s^{-1}}$) within the uncertainties (Table 3). Similar statistics are obtained for the $EW \geq$0.5Å narrow absorbers.

(3) More strongly absorbed quasars tend to have redder UV continua, confirming earlier findings based on radio sources only (Baker et al. 2002) and consistent with trends seen for broad absorption line quasars (Brotherton et al. 2001).

(4) Lobe-dominated quasars, believed to be viewed at relatively larger angles to their radio source axis than core-dominated sources, are most frequently and most strongly absorbed in general. While this has been seen previously, the trend was tested here on a well selected subset of radio-loud quasars with a range of source inclinations and with luminosity biases strongly reduced. This solidifies the reality of this trend, indicating a near-equatorial distribution of narrow absorbers.

(5) Among the absorbed radio quasars significant correlations are found between the strength of the absorbers and (a) the UV continuum luminosity (when all detected NALs are analyzed), and (b) the UV spectral slope, such that absorbed radio quasars tend to have redder and fainter UV continua. Combined with item (4) this is interpreted here as an inclination dependent reddening and absorption effect. These effects must dominate radiation pressure effects in these radio sources, since the opposite correlations are otherwise expected.

(6) Absorbed radio-quiet quasars are also redder but stronger narrow absorption is detected in more luminous sources. This supports the picture in which radiation pressure is related to and perhaps responsible for the stronger absorption. This would be expected if increased radiation pressure in more luminous sources generate and accelerate more absorbing outflows by, for example, heating the upper layers of the accretion disk, as advocated in some disk outflow models. Narrow absorption stronger than $EW_{\rm rest} \approx 3$Å is not seen for the radio-quiet quasars.

(7) In addition to a higher incidence of associated

[14] M_V was computed based on the data presented by Ganguly et al. (2001).

C IV absorbers a clustering of absorbers is detected in both radio-loud and radio-quiet quasars at outflow velocities around $-15\,000\,\mathrm{km\,s^{-1}}$ and an increase in absorber strength is seen around $-18\,000\,\mathrm{km\,s^{-1}}$ (Fig. 7). This is intriguingly close to the common terminal velocity (about $-20\,000\,\mathrm{km\,s^{-1}}$) seen for broad absorption line (BAL) outflows. It is here suggested that the intermediate strength absorbers ($EW_{\rm rest} \lesssim 3$Å) may constitute a slightly different population of narrow absorbers, perhaps entrained by BAL outflows in radio-quiet quasars and radio outflows in radio quasars.

(8) The dearth of UV narrow absorbers in "face-on" radio quasars (i.e., core-dominated) reported by Ganguly et al. (2001) for their sample of $z \lesssim 1$ quasars is not supported. In contrast, a strikingly high fraction of $z \approx 2$ radio core-dominated quasars with emission line FWHM(C IV) $\lesssim$6000 $\mathrm{km\,s^{-1}}$ have detected absorption stronger than $EW \geq 0.5$Å (Tables 7; Fig. 10). While redshift evolution of the column density and distribution of the absorbing gas may explain the different results, the sample selection is suspected the main cause, as the $z \lesssim 0.5$ BQS quasars are as strongly absorbed as the quasars here.

(9) The strongest absorption is seen among the radio quasars with the largest extent of the radio emission and the upper envelope in absorption strength decreases with decreasing linear radio size (Fig. 9). This contrasts the results of Baker et al. (2002). For the well defined, homogeneous, low-frequency selected (source inclination unbiased) Molonglo quasar sample they find the strongest narrow associated C IV λ1549 absorption among the most dust-reddened quasars with the smallest linear extent of their radio emission, namely among the compact steep spectrum sources, believed to be young radio sources. Baker et al. propose that the presence and strength of narrow associated absorption is likely related to radio source growth such that smaller (younger) radio sources are more strongly absorbed. Although less homogeneous, the radio quasar sample studied here is well selected with respect to source inclination and intrinsic brightness, and so should not be strongly biased in this regard. The deviating results are at present attributed to the fact that the radio quasars here are intrinsically more luminous by a factor $\geq$10 than the Molonglo quasars, possibly enabling stronger absorbing outflows. However, the small number statistics of both studies may also contribute.

Items (4), (5), and (6) are consistent with expectations of disk-wind scenarios (e.g., Murray & Chiang 1995, 1997) in which the strong X-ray flux in radio-loud quasars overionize the somewhat equatorially outflowing wind to a high degree, thereby significantly reducing the effects of the radiation pressure on the wind. In this case, the stronger associated narrow absorption lines in radio-loud quasar are explained as "failed" broad absorption line outflows. The lack of individual narrow associated absorption systems with $EW_{\rm rest} > 3$Å and the higher frequency of BALs among radio-quiet quasars are also consistent with the purported stronger ability of RQQs to accelerate the outflows.

Many thanks are due to my collaborator and former co-advisor Peter Barthel for allowing me to include the radio-loud quasar data in this follow-up study to my thesis work. I thank Luis Ho for helpful discussions early in the course of this work, and Peter Barthel for comments on the manuscript. The anonymous referee is thanked for careful reading of the manuscript and for helpful comments. Financial support from the Columbus Fellowship is gratefully acknowledged. Part of the observations reported here were obtained at the MMT Observatory, a joint facility of the Smithsonian Institution and the University of Arizona This research has made use of the NASA/IPAC Extragalactic Database (NED) which is operated by the Jet Propulsion Laboratory, California Institute of Technology, under contract with the National Aeronautics and Space Administration.

REFERENCES

Anderson, S. F., Weymann, R. J., Foltz, C. B., & Chaffee, F. H. 1987, AJ, 94, 278
Baker, J. C., Hunstead, R. W., Athreya, R. M., Barthel, P. D., de Silva, E., Lehnert, M. D., & Saunders, R. D. E. 2002, ApJ, 568, 592
Barlow, T. A., Hamann, F., & Sargent, W. L. W. 1997, ASP Conf. Ser. 128: Mass Ejection from Active Galactic Nuclei, ed. N. Arav, I. Shlosman, and R. J. Weymann (San Francisco: ASP), 13
Barthel, P. D. 1989, ApJ, 336, 606
Barthel, P. D., Miley, G. K., Schilizzi, R. T., & Lonsdale, C. J. 1988, A&AS, 73, 515
Barthel, P. D., Tytler, D. R., & Thomson, B. 1990, A&AS, 82, 339
Barthel, P. D., Tytler, D. R., & Vestergaard, M. 1997, in Mass Ejection from Active Galactic Nuclei, eds. N. Arav, I. Shlosman, & R. J. Weymann, (San Francisco: ASP), 48
Barthel, P. D., Vestergaard, M., & Lonsdale, C. J. 2000, A&A, 354, 7
Barvainis, R., Lonsdale, C., & Antonucci, R. 1996, AJ, 111, 1431
Becker, R. H., Gregg, M. D., Hook, I. M., McMahon, R. G., White, R. L., & Helfand, D. J. 1997, ApJ, 479, L93
Becker, R. H., White, R. L., Gregg, M. D., Brotherton, M. S., Laurent-Muehleisen, S. A., & Arav, N. 2000, ApJ, 538, 72
Becker, R. H. et al. 2001, ApJS, 135, 227
Begelman, M. C. 1999, The Most Distant Radio Galaxies, ed. H. J. A. Rttgering, P. N. Best, and M. D. Lehnert, 173
Brandt, W. N., Fabian, A. C., & Pounds, K. A. 1996, MNRAS, 278, 326
Brandt, W. N., Laor, A., & Wills, B. J. 2000, ApJ, 528, 637
Briggs, F. H., Turnshek, D. A., & Wolfe, A. M. 1984, ApJ, 287, 549
Brotherton, M. S., van Breugel, W., Smith, R. J., Boyle, B. J., Shanks, T., Croom, S. M., Miller, L., & Becker, R. H. 1998, ApJ, 505, L7
Brotherton, M. S., Tran, H. D., Becker, R. H., Gregg, M. D., Laurent-Muehleisen, S. A., & White, R. L. 2001, ApJ, 546, 775
Canalizo, G. & Stockton, A. 2001, ApJ, 555, 719
Canalizo, G. & Stockton, A. 2002, ASP Conf. Ser. 255: Mass Outflow in Active Galactic Nuclei: New Perspectives, ed. D. M. Crenshaw, S. B. Kraemer, and I. M. George (San Francisco: ASP), 195
Colla, G. et al. 1970, A&AS, 1, 281
Colla, G. et al. 1972, A&AS, 7, 1
Colla, G. et al. 1973, A&AS, 11, 291
Crenshaw, D. M. & Kraemer, S. B. 2001, ApJ, 562, L29
Crenshaw, D. M., Kraemer, S. B., Boggess, A., Maran, S. P., Mushotzky, R. F., & Wu, C. 1999, ApJ, 516, 750
Elvis, M. 2000, ApJ, 545, 63
Evans, D. W. 1989, A&AS, 78, 249
Foltz, C. B., Chaffee, F. H., Hewett, P. C., Weymann, R. J., & Morris, S. L. 1990, BAAS, 22, 806
Foltz, C. B., Weymann, R. J., Peterson, B. M., Sun, L., Malkan, M. A., & Chaffee, F. H. 1986, ApJ, 307, 504
Foltz, C. B., et al. 1988, in QSO Absorption Lines: Probing the Universe, ed. C. Blades, D. Turnshek, & C. Norman (Cambridge: CUP), 53
Francis, P. J., Hooper, E. J., & Impey, C. D. 1993, AJ, 106, 417
Ganguly, R., Bond, N. A., Charlton, J. C., Eracleous, M., Brandt, W. N., & Churchill, C. W. 2001, ApJ, 549, 133

Goodrich, R. W. 2001, Advanced Lectures on the Starburst-AGN Connection, ed. I. Aretxaga, D. Kunth, and R. Mújica (Singapore: World Scientific), 69
Goodrich, R. W. & Miller, J. S. 1995, ApJ, 448, L73
Green, P. J., Aldcroft, T. L., Mathur, S., Wilkes, B. J., & Elvis, M. 2001, ApJ, 558, 109
Gregg, M. D., Becker, R. H., Brotherton, M. S., Laurent-Muehleisen, S. A., Lacy, M., & White, R. L. 2000, ApJ, 544, 142
Gregg, M. D., Becker, R. H., White, R. L., Helfand, D. J., McMahon, R. G., & Hook, I. M. 1996, AJ, 112, 407
Hall, P. B. et al. 2002, ApJS, 141, 267
Hamann, F. 2000, "Intrinsic AGN Absorption Lines", Encyclopedia of Astronomy and
Astrophysics (MacMillan and the Institute of Physics Publishing)
Hamann, F. W., Barlow, T. A., Chaffee, F. C., Foltz, C. B., & Weymann, R. J. 2001, ApJ, 550, 142
Hamann, F., Barlow, T., Cohen, R. D., Junkkarinen, V., & Burbidge, E. M. 1997, ASP Conf. Ser. 128: Mass Ejection from Active Galactic Nuclei, ed. N. Arav, I. Shlosman, and R. J. Weymann (San Francisco: ASP), 19
Hamann, F., Korista, K. T., & Morris, S. L. 1993, ApJ, 415, 541
Hewett, P. C. & Foltz, C. B. 2003, AJ, 125, 1784
Hewett, P. C., Foltz, C. B., & Chaffee, F. H. 1995, AJ, 109, 1498
Hewitt, A. & Burbidge, G. 1993, ApJS, 87, 451
Jannuzi, B. T. et al. 1996, ApJ, 470, L11
Jannuzi, B. T. et al. 1998, ApJS, 118, 1
Kapahi, V. K., Athreya, R. M., Subrahmanya, C. R., Baker, J. C., Hunstead, R. W., McCarthy, P. J., & van Breugel, W. 1998, ApJS, 118, 327
Kukula, M. J., Dunlop, J. S., Hughes, D. H., & Rawlings, S. 1998, MNRAS, 297, 366
Laor, A. & Brandt, W. N. 2002, ApJ, 569, 641
Large, M. I., Mills, B. Y., Little, A. G., Crawford, D. F., & Sutton, J. M. 1981, MNRAS, 194, 693
Longair, M. S. & Riley, J. M. 1979, MNRAS, 188, 625
Lonsdale, C. J., Barthel, P. D., & Miley, G. 1993, ApJS, 87, 63
Najita, J., Dey, A., & Brotherton, M. 2000, AJ, 120, 2859
Ma, F. 2002, MNRAS, 335, L99
Mathur, S., Elvis, M., & Wilkes, B. 1995, ApJ, 452, 230
Mathur, S., Matt, G., Green, P. J., Elvis, M., & Singh, K. P. 2001, ApJ, 551, L13
Mathur, S., Wilkes, B., Elvis, M., & Fiore, F. 1994, ApJ, 434, 493
Miley, G. K. 1971, MNRAS, 152, 477
Murray, N., & Chiang, J. 1995, ApJ, 454, L105
Murray, N. & Chiang, J. 1997, ApJ, 474, 91
Møller, P. & Jakobsen, P. 1987, ApJ, 320, L75
O'Dea, C. P. 1998, PASP, 110, 493
Ogle, P. M., Cohen, M. H., Miller, J. S., Tran, H. D., Goodrich, R. W., & Martel, A. R. 1999, ApJS, 125, 1
Perry, J. J., Burbidge, E. M., & Burbidge, G. R. 1978, PASP, 90, 337
Peterson, B. 1997, An Introduction to Active Galactic Nuclei (Cambridge: CUP)
Prochaska, J. X., Gawiser, E., Wolfe, A. M., Cooke, J., & Gelino, D. 2003, ApJS, 147, 227
Proga, D., Stone, J. M., & Kallman, T. R. 2000, ApJ, 543, 686
Readhead, A. C. S., Taylor, G. B., Xu, W., Pearson, T. J., Wilkinson, P. N., & Polatidis, A. G. 1996, ApJ, 460, 612
Richards, G. T. 2001, ApJS, 133, 53
Richards, G. T., York, D. G., Yanny, B., Kollgaard, R. I., Laurent-Muehleisen, S. A., & vanden Berk, D. E. 1999, ApJ, 513, 576
Sabra, B., Hamann, F., & Shields, J. 2002, American Physical Society, April Meeting, Jointly Sponsored with the High Energy Astrophysics Division (HEAD) of the American Astronomical Society April 20 - 23, 2002 Albuquerque Convention Center Albuquerque, New Mexico Meeting ID: APR02, abstract #D11.007, 11007
Sargent, W. L. W., Boksenberg, A., & Steidel, C. C. 1988, ApJS, 68, 539
Savage, B. D. et al. 2000, ApJS, 129, 563
Schmidt, G. D. & Hines, D. C. 1999, ApJ, 512, 125
Schneider, D. P. et al. 2002, AJ, 123, 567
Spinrad, H., Marr, J., Aguilar, L., & Djorgovski, S. 1985, PASP, 97, 932
Vestergaard, M. 2000, PASP, 112, 1504
Vestergaard, M. 2002, ASP Conf. Ser. 255: Mass Outflow in Active Galactic Nuclei: New Perspectives, ed. D. M. Crenshaw, S. B. Kraemer, and I. M. George (San Francisco: ASP), 143 (Paper I)
Vestergaard, M. 2004a, ApJ, 600, in press
Vestergaard, M. 2004b, ApJ, submitted
Vestergaard, M. & Wilkes, B. J. 2001, ApJS, 134, 1
Vestergaard, M., Wilkes, B. J., & Barthel, P. D. 2000, ApJ, 538, L103
Weymann, R. J., Carswell, R. F., & Smith, M. G. 1981, ARA&A, 19, 41
Weymann, R. J., Morris, S. L., Foltz, C. B., & Hewett, P. C. 1991, ApJ, 373, 23
Weymann, R. J, Williams, R., Peterson, B., Turnshek, D. 1979, ApJ, 234, 33
White, R. L. et al. 2000, ApJS, 126, 133
Wilkes, B. J., Tananbaum, H., Worrall, D. M., Avni, Y., Oey, M. S., & Flanagan, J. 1994, ApJS, 92, 53
Wills, B. J., & Brotherton, M. S., 1995, ApJ, 448, L81
Wills, B. J. et al. 1995, ApJ, 447, 139
Wright, A, & Otrupcek, R. 1990, Parkes Catalogue, Australia Telescope National Facility, A. Wright & R. Otrupcek, (Eds)
Young, P., Sargent, W. L. W., & Boksenberg, A. 1982, ApJS, 48, 455

TABLE 1
PROPERTIES OF ABSORBED QUASARS AND THEIR ABSORBERS

Object	Radio-type	z	M_V [mag]	$\log L_\lambda(1550\text{Å})$ [erg s^{-1}]	α_λ	$\lambda_{\rm obs}$ [Å]	$z_{\rm abs}$	v [km s^{-1}]	β	$EW_{\rm abs}$ [Å]	$\sigma(EW)$ [Å]
(1)	(2)	(3)	(4)	(5)	(6)	(7)	(8)	(9)	(10)	(11)	(12)
Q0000−001	RQ	2.576	−27.18	43.430	-1.30 ± 0.14	5543.8	2.5790	241	−0.0008	0.50	0.03
						5512.5	2.5587	−1458	0.0049	0.91	0.03
Q0008−008	RQ	2.051	−27.18	43.201	-1.42 ± 0.21	4600.6	1.9701	−8014	0.0267	0.94	0.05
Q0017+154	LDQ	2.015	−28.30	43.994	-1.64 ± 0.09	4450.7	1.8733	−14437	0.0482	1.26	0.09
						4550.7	1.9378	−7789	0.0260	0.50	0.09
Q0106+013	CDQ	2.100	−28.21	43.433	-2.06 ± 0.21	4799.2	2.0983	−169	0.0006	0.46	0.02
Q0107−005	RQ	1.749	−27.25	43.079	-1.92 ± 0.48	4264.3	1.7530	417	−0.0014	1.26	0.05
Q0109+176	LDQ	2.152	−27.90	43.650	-1.36 ± 0.31	4889.0	2.1562	452	−0.0015	4.77	0.06
						4620.5	1.9829	−16466	0.0549	0.52	0.11
Q0225−014	LDQ	2.039	−27.94	43.481	-1.77 ± 0.25	4642.7	1.9972	−4174	0.0139	1.39	0.08
Q0226−038	CDQ	2.060	−29.60	43.798	-1.79 ± 0.15	4713.8	2.0431	−1631	0.0054	0.38	0.03
Q0244+017	RQ	1.948	−27.13	43.159	-1.15 ± 0.25	4588.4	1.9622	1397	−0.0047	2.99	0.04
Q0252+016	RQ	2.457	−28.51	44.104	-1.27 ± 0.11	5108.9	2.2982	−14120	0.0471	0.35	0.04
Q0253−024	RQ	1.986	−27.14	43.176	-1.51 ± 0.33	4533.0	1.9264	−6001	0.0200	0.81	0.07
Q0254−016	RQ	2.685	−27.86	43.601	-1.52 ± 0.28	5449.6	2.5181	−13852	0.0462	0.70	0.07
Q0258+021	RQ	2.521	−28.85	43.955	-2.11 ± 0.12	5477.0	2.5358	1237	−0.0041	0.17	0.02
Q0317−023	CDQ	2.076	−27.08	42.764	-1.03 ± 0.43	4743.8	2.0625	−1289	0.0043	1.39	0.05
Q0348+061	RQ	2.058	−28.95	43.771	-0.79 ± 0.10	4399.3	1.8401	−22093	0.0737	0.56	0.05
						4595.5	1.9668	−9052	0.0302	0.69	0.05
						4682.2	2.0227	−3450	0.0115	1.26	0.03
						4696.0	2.0316	−2568	0.0086	0.76	0.03
Q0445+097	CSS	2.106	−26.99	42.923	-1.12 ± 0.60	4811.8	2.1064	16	−0.0001	4.43	0.08
						4820.1	2.1118	533	−0.0018	2.22	0.08
Q0458−020	CDQ	2.286	−27.03	43.431	-0.20 ± 0.18	4706.0	2.0381	−23437	0.0782	1.50	0.11
						4783.2	2.0879	−18585	0.0620	0.63	0.11
Q0504+030	LDQ	2.470	−27.74	43.389	-1.63 ± 0.33	5280.1	2.4087	−5364	0.0179	1.15	0.10
Q0751+298	CSS	2.106	−28.10	44.054	-2.33 ± 0.21	4519.7	1.9178	−18688	0.0623	0.69	0.08
Q0802+103	LDQ	1.952	−28.11	43.939	-1.80 ± 0.20	4568.4	1.9492	−289	0.0010	6.17	0.02
Q0805+046	CDQ	2.876	−29.24	44.409	-2.26 ± 0.09	6004.0	2.8761	32	−0.0001	0.27	0.02
Q0808+289	LDQ	1.886	−27.99	43.858	-1.17 ± 0.14	4307.1	1.7805	−11171	0.0373	0.45	0.06
						4450.0	1.8728	−1391	0.0046	2.32	0.05
Q0831+101	LDQ	1.757	−26.47	42.835	-1.48 ± 0.53	4274.7	1.7596	284	−0.0009	0.88	0.09
						4243.0	1.7392	−1947	0.0065	0.96	0.10
Q0835+580	LDQ	1.528	−28.12	43.259	-0.27 ± 0.11	3922.3	1.5321	530	−0.0018	1.24	0.07
						3937.5	1.5420	1696	−0.0057	1.57	0.07
Q0941+261	CSS	2.906	−29.58	43.840	-2.67 ± 0.29	6064.2	2.9149	684	−0.0023	0.33	0.06
Q1016−006	RQ	2.181	−27.87	43.541	-1.80 ± 0.14	4573.2	1.9524	−22355	0.0746	1.38	0.04
Q1023+067	LDQ	1.698	−27.48	43.188	-0.90 ± 0.19	4204.1	1.7141	1742	−0.0058	7.59	0.06

TABLE 1—*Continued*

Object	Radio-type	z	M_V	$\log L_\lambda(1550\text{Å})$	α_λ	$\lambda_{\rm obs}$	$z_{\rm abs}$	v	β	$EW_{\rm abs}$	$\sigma(EW)$
...	...	...	[mag]	[erg s^{-1}]	...	[Å]	...	[km s^{-1}]	...	[Å]	[Å]
(1)	(2)	(3)	(4)	(5)	(6)	(7)	(8)	(9)	(10)	(11)	(12)
Q1045+052	RQ	2.120	−27.38	43.297	-1.44 ± 0.22	4535.9	1.9283	−18946	0.0632	1.62	0.07
Q1116+128	CDQ	2.124	−27.29	43.590	-1.69 ± 0.15	4845.0	2.1279	399	−0.0013	1.91	0.03
						4611.1	1.9768	−14424	0.0481	0.84	0.05
Q1158+122	LDQ	2.014	−28.90	43.864	-1.27 ± 0.10	4642.0	1.9968	−1683	0.0056	1.10	0.04
Q1208+105	RQ	1.864	−27.80	42.841	-1.20 ± 0.59	4431.5	1.8609	−278	0.0009	1.66	0.10
Q1219+491	RQ	2.323	−27.70	43.484	-1.62 ± 0.18	4929.3	2.1822	−12955	0.0432	0.58	0.08
						5031.1	2.2480	−6834	0.0228	1.30	0.08
Q1223+178	RQ	2.930	−29.48	44.224	-1.43 ± 0.23	5661.0	2.6546	−21715	0.0724	0.75	0.05
						6037.4	2.8976	−2454	0.0082	1.12	0.04
						6130.2	2.9575	2118	−0.0071	1.62	0.04
Q1226+105	LDQ	2.303	−28.04	44.442	-2.65 ± 0.11	4790.2	2.0924	−19695	0.0657	0.41	0.07
Q1227+120	RQ	2.440	−27.54	43.310	-0.93 ± 0.22	5380.2	2.4734	2883	−0.0096	0.75	0.10
Q1230+164	RQ	2.716	−29.41	44.329	-1.48 ± 0.10	5713.2	2.6883	−2256	0.0075	0.82	0.04
						5738.7	2.7048	−923	0.0031	2.37	0.03
Q1232−004	RQ	1.587	−26.65	42.859	-1.70 ± 0.29	3837.4	1.4774	−12953	0.0432	0.92	0.08
Q1246−022	RQ	2.109	−28.49	43.911	-1.43 ± 0.08	4473.4	1.8880	−22058	0.0736	0.93	0.04
Q1259+344	RQ	2.754	−28.33	43.752	-0.99 ± 0.14	5706.7	2.6841	−5670	0.0189	1.13	0.04
						5780.6	2.7318	−1813	0.0060	2.15	0.03
						5841.0	2.7708	1306	−0.0044	3.44	0.03
Q1313+200	CDQ	2.462	−28.26	43.985	-1.88 ± 0.08	5373.0	2.4687	570	−0.0019	1.98	0.03
Q1323+655	LDQ	1.624	−28.15	44.538	-2.88 ± 0.16	4043.3	1.6102	−1527	0.0051	0.41	0.05
Q1402−012	CDQ	2.518	−28.67	43.968	-2.23 ± 0.16	5226.9	2.3744	−12447	0.0415	0.37	0.08
Q1409+095	RQ	2.840	−28.89	43.933	-2.19 ± 0.38	5679.2	2.6663	−13839	0.0462	0.72	0.07
						5762.8	2.7203	−9465	0.0316	0.87	0.06
Q1434−009	RQ	1.669	−27.71	43.432	-1.73 ± 0.14	3966.8	1.5609	−12408	0.0414	0.56	0.05
						3969.1	1.5624	−12231	0.0408	0.56	0.05
Q1443−010	RQ	1.795	−27.82	43.594	-0.95 ± 0.13	4308.3	1.7814	−1421	0.0047	1.67	0.04
Q1540+180	LDQ	1.663	−27.90	43.277	-2.46 ± 0.33	3940.1	1.5436	−13679	0.0456	0.68	0.10
Q1606+289	LDQ	1.983	−27.46	43.326	-1.15 ± 0.21	4600.0	1.9697	−1372	0.0046	9.11	0.16
Q1614+051	GPS	3.212	−27.73	43.850	-1.73 ± 0.10	6344.3	3.0957	−8400	0.0280	0.41	0.04
						6128.9	2.9567	−18732	0.0625	0.41	0.04
Q1629+120	CSS	1.781	−27.63	43.306	-2.09 ± 0.32	4363.3	1.8169	3869	−0.0129	0.81	0.07
Q1629+680	CSS	2.473	−27.78	43.581	-2.44 ± 0.20	5401.6	2.4872	1255	−0.0042	0.33	0.04
Q1633+382	CDQ	1.810	−28.06	44.056	-0.87 ± 0.05	4096.3	1.6445	−18133	0.0605	0.30	0.02
Q1656+477	CDQ	1.614	−27.84	43.804	-1.86 ± 0.18	3895.4	1.5148	−11585	0.0386	0.77	0.05
Q1658+575	LDQ	2.171	−28.38	43.640	-1.93 ± 0.13	4931.8	2.1839	1196	−0.0040	0.27	0.03
Q1701+379	LDQ	2.454	−27.75	43.372	-2.52 ± 0.40	5311.6	2.4291	−2187	0.0073	0.52	0.07
						4909.0	2.1692	−25753	0.0859	0.81	0.11

TABLE 1—*Continued*

Object	Radio-	z	M_V	$\log L_\lambda(1550\text{Å})$	α_λ	$\lambda_{\rm obs}$	$z_{\rm abs}$	v	β	$EW_{\rm abs}$	$\sigma(EW)$
...	type	...	[mag]	[erg s^{-1}]	...	[Å]	...	[km s^{-1}]	...	[Å]	[Å]
(1)	(2)	(3)	(4)	(5)	(6)	(7)	(8)	(9)	(10)	(11)	(12)
Q1726+344	CSS	2.426	−28.20	43.768	-2.05 ± 0.08	5204.6	2.3600	−6000	0.0200	2.00	0.05
Q2048+196	CDQ	2.364	−28.11	43.620	-1.84 ± 0.15	5193.3	2.3527	−1049	0.0035	1.07	0.04
Q2150+053	LDQ	1.979	−28.55	43.767	-1.33 ± 0.12	4630.7	1.9895	1013	−0.0034	0.62	0.03
Q2222+051	LDQ	2.322	−28.06	43.754	$+0.51 \pm 0.28$	5129.6	2.3115	−973	0.0032	1.23	0.04
						4848.3	2.1300	−17857	0.0596	2.38	0.06
Q2251+244	CSS	2.313	−28.36	43.773	-1.41 ± 0.12	4887.9	2.1555	−14601	0.0487	1.47	0.07
						5192.3	2.3520	3498	−0.0117	0.92	0.06
						5210.6	2.3639	4554	−0.0152	2.35	0.07
Q2351+022	RQ	2.024	−27.91	43.473	-1.34 ± 0.23	4702.7	2.0360	1158	−0.0039	2.26	0.06
Q2359+002	RQ	2.675	−27.35	43.475	-2.98 ± 0.24	5697.5	2.6782	291	−0.0010	2.42	0.04

Note. — col (1): Quasar name; col (2): Radio type: RQ= radio quiet quasar, CDQ= core-dominated quasar, LDQ= lobe-dominated quasar, CSS= compact steep-spectrum source, GPS = Giga-hertz Peaked spectrum source (see § 2); col (3): Quasar redshift; col (4): Absolute V-band magnitude ($\alpha = -0.7$ was adopted for the K-correction; $F_\lambda \propto \lambda^{\alpha_\lambda}$); col (5): logarithm of the monochromatic continuum luminosity at 1550Å; col (6): UV spectral slope, α_λ; col (7): Wavelength position of the narrow absorber in the observed frame of reference; col (8): Redshift of the absorber; col (9): Absorber velocity defined here as $v = -\beta c$. That is, negative velocities denote blueshifted absorbers relative to the emission line redshift. Since UV broad emission lines can be blueshifted relative to the systemic redshift, redshifted absorption need not indicate infall toward the central engine; col (10): $\beta = (r^2 - 1)/(r^2 + 1)$ where $r = (1 + z_{\rm em})/(1 + z_{\rm abs})$, and c is the speed of light (Weymann et al. 1979; Peterson 1997); col (11): Restframe equivalent width of the narrow absorber; col (12): The $1\,\sigma$ *EW* uncertainty measured from the continuum *rms* across a resolution element at the position of the absorber.

TABLE 2
PROPERTIES OF UNABSORBED QUASARS

Object	Radio-type	z	M_V [mag]	$\log L_\lambda(1550\text{Å})$ [erg s^{-1}]	α_λ
...	...	...	...	...	...
(1)	(2)	(3)	(4)	(5)	(6)
Q0002−008	RQ	2.166	−28.56	43.561	-2.47 ± 0.26
Q0003−006	RQ	1.723	−26.46	43.127	-1.67 ± 0.20
Q0015+026	RQ	2.468	−28.06	43.428	$-1.62\ ^{+\ 0.42}_{-\ 0.50}$
Q0020+022	RQ	1.788	−27.53	43.362	-2.27 ± 0.20
Q0038−019	LDQ	1.672	−27.42	43.893	-2.22 ± 0.14
Q0040−017	RQ	2.398	−28.70	44.159	-1.90 ± 0.25
Q0115−011	RQ	2.179	−28.28	43.518	-1.89 ± 0.35
Q0206+293	CDQ	2.197	−27.54	43.169	-1.88 ± 0.23
Q0238+100	LDQ	1.829	−28.19	43.587	$-1.54\ ^{+\ 0.40}_{-\ 0.51}$
Q0352+123	LDQ	1.616	−26.53	43.166	-1.11 ± 0.29
Q0730+257	LDQ	2.688	−27.20	43.787	-2.12 ± 0.30
Q0758+120	LDQ	2.658	−27.16	43.677	-2.56 ± 0.22
Q0856+124	CSS	1.767	−26.69	43.058	$-2.35\ ^{+\ 0.47}_{-\ 0.63}$
Q0926+117	LDQ	1.754	−26.96	43.698	-2.17 ± 0.16
Q1020+014	RQ	1.605	−27.70	43.386	-1.57 ± 0.25
Q1043+071	RQ	2.115	−27.3	43.187	-1.68 ± 0.25
Q1046+058	RQ	1.971	−27.74	43.470	-1.67 ± 0.15
Q1055+499	CSS	2.387	−26.65	43.551	-2.29 ± 0.25
Q1137+305	RQ	1.584	−28.89	43.971	-1.60 ± 0.06
Q1138+002	RQ	1.760	−27.46	43.147	-1.81 ± 0.19
Q1146+111	RQ	1.932	−27.46	43.448	-1.40 ± 0.09
Q1214+106	LDQ	1.881	−27.79	43.450	$-2.64\ ^{+\ 0.58}_{-\ 0.84}$
Q1221+113	CSS	1.759	−27.28	44.008	-2.37 ± 0.14
Q1237+134	RQ	1.722	−28.21	43.727	-1.33 ± 0.08
Q1258+404	LDQ	1.667	−26.51	43.142	$-2.41\ ^{+\ 0.48}_{-\ 0.64}$
Q1311−270	LDQ	2.196	−29.14	44.305	-2.17 ± 0.19
Q1330+011	RQ	3.501	−29.34	43.863	$-3.86\ ^{+\ 0.39}_{-\ 0.51}$
Q1402+044	CDQ	3.205	−28.43	43.678	-2.20 ± 0.24
Q1440−004	RQ	1.811	−27.45	43.568	-1.61 ± 0.14
Q1442+101	GPS	3.527	−30.30	44.376	-1.24 ± 0.09
Q1517+239	RQ	1.833	−27.78	43.497	-1.26 ± 0.14
Q1542+042	CDQ	2.182	−28.56	43.701	-1.59 ± 0.32
Q1554−203	LDQ	1.938	−27.20	43.464	-1.88 ± 0.27
Q1556−245	CDQ	2.810	−28.23	43.631	-1.52 ± 0.26
Q1602+576	CSS	2.854	−29.20	44.781	-3.31 ± 0.15
Q1607+183	CDQ	3.097	−28.84	43.941	-2.33 ± 0.23
Q1634+406	RQ	1.730	−27.38	43.313	$-2.36\ ^{+\ 0.36}_{-\ 0.46}$
Q1638+390	RQ	2.374	−28.11	43.736	-1.43 ± 0.14
Q1702+298	CSS	1.928	−27.27	42.690	-2.00 ± 0.00
Q1704+710	RQ	2.010	−28.99	43.788	-1.06 ± 0.11
Q1705+018	GPS	2.571	−28.06	43.540	$-2.21\ ^{+\ 0.50}_{-\ 0.67}$
Q1816+475	LDQ	2.221	−28.30	43.792	-2.41 ± 0.20
Q1857+566	LDQ	1.576	−28.48	43.663	-2.33 ± 0.12
Q2158+101	CSS	1.727	−28.32	43.328	-1.70 ± 0.18
Q2212−299	CDQ	2.702	−29.92	44.341	-2.46 ± 0.07
Q2223+210	CDQ	1.947	−28.61	43.975	-2.53 ± 0.19
Q2233+136	RQ	3.210	−27.22	43.812	-4.25 ± 0.09
Q2239+007	RQ	2.412	−26.72	43.391	-2.00 ± 0.19
Q2248+192	LDQ	1.794	−27.64	43.236	-1.60 ± 0.28
Q2334+019	RQ	2.185	−27.54	43.705	-1.36 ± 0.18
Q2341+010	RQ	2.305	−27.00	42.888	$-1.65\ ^{+\ 0.64}_{-\ 0.77}$
Q2345+061	CSS	1.538	−27.93	43.384	-1.76 ± 0.16
Q2350−007	RQ	1.617	−27.23	43.228	-0.70 ± 0.20

Note. — colums (1) − (6): see notes to Table 1.

TABLE 3
FREQUENCY OF C IV NAL ABSORBED OBJECTS[a]

Sample (1)	No. of QSOs (2)	No. of Absorbed Quasars with |Abs. Vel.| ≤ 21000 km s^{-1} (3)		No. of Quasars with |Absorber Velocity| ≤ 5000 km s^{-1} (4)	No. of Quasars with 5000 < |Absorber Velocity| ≤ 21000 km s^{-1} (5)
		All EWs	Doublet $EW \geq 0.5$Å[b]		
All QSOs	114	59±7.7; 52± 7%	45±6.7; 39± 5%	31±5.6; 27± 5%	21±4.6; 18± 4%
RQQ	48	22±4.7; 46±10%	19±4.4; 40± 9%	12±3.5; 25± 7%	10±3.2; 21± 7%
RLQ	66	37±6.1; 56± 9%	26±5.1; 39± 7%	19±4.4; 29± 7%	11±3.3; 17± 5%
CDQ	18	11±3.3; 61±18%	6±2.4; 33±13%	4±2.0; 22±11%	3±1.7; 17±10%
LDQ	31	18±4.2; 58±14%	15±3.9; 48±12%	12±3.5; 80±23%	5±2.2; 33±15%
CSS	14	7±2.6; 50±19%	5±2.2; 36±16%	3±1.7; 21±12%	3±1.7; 21±12%
CSS+GPS	17	8±2.8; 47±17%	5±2.2; 29±13%	3±1.7; 18±10%	3±1.7; 18±10%
		Strongly Absorbed Quasars[c]			
All QSOs	114	40±6.3; 35± 5%		28±5.3; 25± 5%	10±3.2; 9± 3%
RQQ	48	15±3.9; 31± 8%		11±3.3; 23± 7%	5±2.2; 10± 5%
RLQ	66	25±5.0; 38± 8%		17±4.1; 26± 6%	5±2.2; 8± 3%
CDQ	18	5±2.2; 28±12%		4±2.0; 22±11%	0±0.0; 0± 0%
LDQ	31	14±3.7; 45±12%		10±3.2; 32±10%	3±1.7; 10± $^{5}_{6}$%
CSS	14	5±2.2; 36±16%		2±1.4; 14±10%	2±1.4; 14±10%
CSS+GPS	17	5±2.2; 29±13%		2±1.4; 12± 8%	2±1.4; 12± 8%
		Weakly Absorbed Quasars[d]			
All QSOs	114	24±4.9; 21± 4%		11±3.3; 10± 3%	13±3.6; 11± 4%
RQQ	48	7±2.6; 15± 5%		2±1.4; 4± 3%	5±2.2; 10± 5%
RLQ	66	17±4.1; 26± 6%		9±3.0; 14± 4%	8±2.8; 12± 4%
CDQ	18	7±2.6; 39±14%		3±1.7; 17±10%	4±2.0; 22±11%
LDQ	31	5±2.2; 16± 7%		3±1.7; 10± 6%	2±1.4; 6± $^{5}_{4}$%
CSS	14	4±2.0; 29±14%		3±1.7; 21±13%	1±1.0; 7± 7%
CSS+GPS	17	5±2.2; 29±13%		3±1.7; 18±10%	2±1.4; 12± 8%

a Number of absorbed quasars and counting errors. The frequency of absorbed quasars include the uncertainties corresponding to the counting errors.
b The most complete subset of absorbed quasars have individual C IV doublet absorbers with $EW_{\rm rest}$ ≥0.5Å and absolute velocity ≤ 21 000 km s^{-1}. See text and Figure 1.
c For each velocity bin, the summed absorption $EW_{\rm rest}$ for each quasar must be at least 1Å to be counted. An individual quasar can have strong high and low velocity absorption and so be counted twice; this is, however, only seen in a couple of cases.
d The summed absorption $EW_{\rm rest}$ for each quasar must be less than 1Å to be counted. This is mainly for comparison with studies finding only weak absorbers. Note that individual absorbers with EW < 0.5Å are included here.

TABLE 4
ABSORBER FREQUENCY AMONG ABSORBED QUASARS ONLY

Sample (1)	Number of Absorbers[a] (#Absrs) (All Abs. Vel's) (2)		#Absrs[a] for |Abs. Velocity| $\leq$ 21000 km s^{-1} (3)	#Absrs[a] for |Abs. Velocity| $\leq$ 5000 km s^{-1} (4)	#Absrs[a] for 5000 < |Absorber Velocity| $\leq$ 21000 km s^{-1} (5)
	All *EW*s	Doublet *EW* $\geq$ 0.5Å[b]			
All QSOs	86±9.3	71±8.4	65±8.1	40±6.3; 62± 9%	25±5.0; 38± 7%
RQQ	36±6.0	34±5.8	30±5.5	17±4.1; 57±13%	13±3.6; 43±12%
RLQ	50±7.1	37±6.1	35±5.9	23±4.8; 66±13%	12±3.5; 34±10%
CDQ	13±3.6	8±2.8	7±2.6	4±2.0; 57±28%	3±1.7; 43±24%
LDQ	25±5.0	21±4.6	20±4.5	14±3.7; 70±18%	6±2.4; 30±12%
CSS	10±3.2	8±2.8	8±2.8	5±2.2; 63±28%	3±1.7; 38±21%
CSS+GPS	12±3.5	8±2.8	8±2.8	5±2.2; 63±28%	3±1.7; 38±21%
	Strong Absorbers[c]				
All QSOs	39±6.2		37±6.1	29±5.4; 78±14%	8±2.8; 22± 8%
RQQ	16±4.0		15±3.9	12±3.5; 80±23%	3±1.7; 20±11%
RLQ	23±4.8		22±4.7	17±4.1; 77±18%	5±2.2; 23±10%
CDQ	5±2.2		4±2.0	4±2.0; 100±50%	0±0.0; 0± 0%
LDQ	13±3.6		13±3.6	10±3.2; 77^{+32}_{-18}%	3±1.7; 23±17%
CSS	5±2.2		5±2.2	3±1.7; 60±34%	2±1.4; 40±28%
CSS+GPS	5±2.2		5±2.2	3±1.7; 60±34%	2±1.4; 40±28%

a Number of absorbers and counting errors. The frequency of absorbers include the uncertainties corresponding to the counting errors.
b Absorbers with $EW_{\rm rest}$ $\geq$0.5Å reach the highest completeness level ($\sim$95%); see § 3.3 and Figure 1.
c Strong absorbers only: summed restframe *EW* per quasar $\geq$ 1.0Å.

TABLE 5
CORRELATION TEST STATISTICS

Independent Parameter (1)	Dependent Parameter (2)	Sample[a] (3)	All NALs Spearman's r (4)	All NALs P^b (%) (5)	NAL $EW \geq 0.5$Å[c] Spearman's r (6)	NAL $EW \geq 0.5$Å[c] P (%) (7)
EW[d]	$\alpha_{\rm UV,\lambda}$	All QSOs	0.53	< 0.01	0.45	0.2
		RQQs	0.32	12.9	0.33	13.0
		RLQs	0.62	0.02	0.56	0.5
EW	M_V	All QSOs	0.23	8.2	-0.12	43.2
		RQQs	-0.23	27.5	-0.43	4.9
		RLQs	0.47	0.5	0.21	29.5
EW	$L_{\rm cont}$	All QSOs	-0.24	6.4	0.13	38.9
		RQQs	0.15	48.4	0.40	7.1
		RLQs	-0.41	1.5	-0.15	46.1

a There are 24 absorbed RQQs (22 with $EW \geq 0.5$Å) and 37 absorbed RLQs (26 with $EW \geq 0.5$Å).
b Probability that no correlation is present.
c Here only quasars with $EW \geq 0.5$Å NALs are analyzed.
d This is the total EW for each quasar.

TABLE 6
SAMPLE COMPARISONS[a]

Sample (1)	M_V range (mag) (2)	$< M_V >$ (mag) (3)	log [L_ν(408MHz) /W Hz^{-1}] range (4)	log [$< L_\nu$(408MHz)$>$ /W Hz^{-1}] (5)
Current RLQ sample	-25.5 to -28.2	-26.7	28.9 to 30.3	29.6
Baker[b] et al. (2002)	-23.0 to -28.2	-25.3	28.1 to 29.0	28.5
Ganguly et al. (2001)	-23.5 to -28.1	-26.2	....	....

a Cosmology adopted: $H_0 = 50$ km s^{-1}Mpc^{-1}, $q_0 = 0.5$, and $\Lambda = 0$.
b The data presented by Kapahi et al. (1998) were used to compute the luminosities for the high-z quasar sample studied by Baker et al. (2002). The B_J magnitudes were converted to V magnitudes as follows: the color correction $B - B_J = 0.24(B - V)$ of Evans (1989) combined with the average $(B - V) = 0.28$ of the Hewitt & Burbidge (1993) quasars with $0.7 \leq z \leq 3.0$ shows that, on average, $B = B_J + 0.07$ and $V = B_J - 0.21$.

TABLE 7
HIGH- AND LOW-VELOCITY ABSORPTION FREQUENCY IN NARROW AND BROAD LINE QUASARS[a]

	|Absorber Vel.| $\leq$ 5000 km s^{-1}			|Absorber Vel.| $>$ 5000 km s^{-1}		
Sample	N	N (FW[b] $\geq$ 6000 km s^{-1})	N (FW $<$ 6000 km s^{-1})	N	N (FW $\geq$ 6000 km s^{-1})	N (FW $<$ 6000 km s^{-1})
(1)	(2)	(3)	(4)	(5)	(6)	(7)
			Number of absorbed quasars and counting errors			
RQQ	12±3.5	6±2.4; 50±20%	6±2.4; 50±20%	10±3.2	2±1.4; 20±14%	8±2.8; 80±28%
RLQ	19±4.4	5±2.2; 26±12%	14±3.7; 74±19%	11±3.3	3±1.7; 27±15%	8±2.8; 73±25%
CDQ	4±2.0	0±0.0; 0± 0%	4±2.0; 100±50%	3±1.7	1±1.0; 33±33%	2±1.4; 66±46%
LDQ	12±3.5	4±2.0; 33±17%	8±2.8; 66±24%	5±2.2	1±1.0; 20±20%	4±2.0; 80±40%
CSS	3±1.7	1±1.0; 33±33%	2±1.4; 66±46%	3±1.7	1±1.0; 33±33%	2±1.4; 66±46%
CSS+GPS	3±1.7	1±1.0; 33±33%	2±1.4; 66±46%	3±1.7	1±1.0; 33±33%	2±1.4; 66±46%
			Number of absorbers and counting errors			
RQQ	17±4.1	9±3.3; 53±19%	8±2.8; 47±17%	13±3.6	2±1.4; 15±11%	11±3.3; 85±25%
RLQ	23±4.8	8±2.8; 35±12%	15±3.9; 65±17%	12±3.5	3±1.7; 25±14%	9±3.0; 75±25%
CDQ	4±2.0	0±0.0; 0± 0%	4±2.0; 100±50%	3±1.7	1±1.0; 33±33%	2±1.4; 66±47%
LDQ	14±3.7	6±2.4; 43±17%	8±2.8; 57±20%	6±2.4	1±1.0; 17±17%	5±2.2; 83±37%
CSS	5±2.2	2±1.4; 40±28%	3±1.7; 60±34%	3±1.7	1±1.0; 33±33%	2±1.4; 66±47%
CSS+GPS	5±2.2	2±1.4; 40±28%	3±1.7; 60±34%	3±1.7	1±1.0; 33±33%	2±1.4; 66±47%

a Note: The statistics in this table are based only on absorbers with restframe $EW \geq 0.5$Å and $|$ abs. vel. $| \leq 21\,000$ km s^{-1}, the most complete subset of absorbers (see § 3.3). Note that quasars with both high and low velocity absorbers will be counted both in columns 2 and 5. Hence, the sum of the entries in these columns may exceed the number of absorbed quasars listed in Tables 3 (top section, column 3 right) and 8 (columns 6 and 7).
b FWHM of the C IV *emission* line.

TABLE 8
FREQUENCY OF ABSORBED AND NON-ABSORBED NARROW AND BROAD LINE QUASARS[a]

	# QSOs	# QSOs	Non-Absorbed Quasars		Absorbed Quasars	
Sample	(NL[b])	(BL[c])	# QSOs (NL)	# QSOs (BL)	# QSOs (NL)	# QSOs (BL)
(1)	(2)	(3)	(4)	(5)	(6)	(7)
All QSOs	91	23	58±7.6; 64± 8%	11±3.3; 48±15%	33±5.7; 36± 6%	12±3.5; 52± 15%
RQQ	34	14	21±4.6; 62±13%	8±2.8; 57±20%	13±3.6; 38±10%	6±2.4; 43± 17%
RLQ	57	9	37±6.1; 65±11%	3±1.7; 33±19%	20±4.5; 35± 8%	6±2.4; 66± 26%
CDQ	15	3	10±3.2; 67±21%	2±1.4; 66±46%	5±2.2; 33±15%	1±1.0; 33± 33%
LDQ	27	4	16±4.0; 59±15%	0±0.0; 0± 0%	11±3.3; 41±12%	4±2.0; 100± 50%
CSS	13	1	9±3.0; 69±23%	0±0.0; 0± 0%	4±2.0; 31±15%	1±1.0; 100±100%
CSS+GPS	16	2	11±3.3; 69±20%	1±1.0; 50±50%	4±2.0; 27±13%	1±1.0; 100± 50%

a Here a quasar is considered to be absorbed if the individual C IV absorption doublets has restframe $EW \geq 0.5$ Å and its absolute velocity is less than 21 000 km s^{-1} (the most complete subset of absorbers; see text). As a result those quasars *with* C IV absorption which does not satisfy these conditions are here counted as non-absorbed.
b NL: Quasars with narrow *emission* lines: FWHM(C IV) $<$ 6000 km s^{-1}.
c BL: Quasars with broad *emission* lines: FWHM(C IV) $\geq$6000 km s^{-1}.